Groundwater seepage into northern San Francisco Bay: Implications for dissolved metals budgets

Glenn A. Spinelli and Andrew T. Fisher
Earth Sciences Department, University of California, Santa Cruz, California, USA

C. Geoffrey Wheat
Global Undersea Research Unit, University of Alaska Fairbanks, Fairbanks, Alaska, USA

Michael D. Tryon and Kevin M. Brown
Scripps Institution of Oceanography, University of California, San Diego, La Jolla, California, USA

A. Russell Flegal
Environmental Toxicology Department, University of California, Santa Cruz, California, USA

Received 6 August 2001; revised 27 February 2002; accepted 4 March 2002; published XX Month 2002.

[1] Nonconservative excesses of dissolved metals in northern San Francisco Bay indicate that there are internal sources of metals within the bay. We quantified groundwater seepage and bioirrigation rates in this area to determine their roles in transporting dissolved metals from benthic sediments to surface waters. We deployed seepage meters and collected sediment, pore water, and bottom water samples at three sites. We determined seepage rates from seepage meters and modeled the transport of water through the sediment using pore water data to constrain rates of diffusion, advection, and bioirrigation. A groundwater flow model incorporating sediment physical properties and local topography constrains more regional seepage estimates. The seepage meters indicate upflow rates from 7 to 56 cm yr^{-1} in March and April 1999 with some large ($\leq$50 cm yr^{-1}) daily fluctuations that greatly exceed predictions based on sediment physical properties and tidally induced pore pressure variations. During this period, results from modeling pore water chemical data are consistent with a small bioirrigation rate ($<1.5 \times 10^{-7}$ s^{-1}) relative to values determined for southern San Francisco Bay, and an average groundwater upwelling speed of 15 cm yr^{-1}. The speed and direction of flow changed throughout the year, with best fits to the data ranging from 20 cm yr^{-1} upflow to 34 cm yr^{-1} downflow and averaging 4 cm yr^{-1} upflow. Confidence intervals (95%) are about $\pm$10 cm yr^{-1} for this method, yet the range of acceptable seepage rates for temporally successive periods only overlap in one of four cases, suggesting that temporal variability can be discerned from potential artifacts. Groundwater flow modeling suggests that the seepage rates determined at our sites represent $\sim$45% of the average seepage rate for the area, applying one consolidation and permeability relationship to all sediments. If we apply these approximations to all of northern San Francisco Bay, benthic fluxes of dissolved metals to the surface waters could account for a relatively large amount ($\leq$60%) of the unknown sources of dissolved cobalt and a relatively small amount ($\leq$4%) of the unknown sources of dissolved silver, cadmium, copper, nickel, and zinc. More focused groundwater discharge or elevated metals concentrations are required to have a larger impact on trace element budgets in this setting. *INDEX TERMS:* 1832 Hydrology: Groundwater transport; 4235 Oceanography: General: Estuarine processes; 1050 Geochemistry: Marine geochemistry (4835, 4850); *KEYWORDS:* groundwater, San Francisco Bay, pore water, dissolved metal, sediment-water interface

1. Introduction

[2] The flow of groundwater into estuaries, lakes, and coastal zones can transport nutrients and contaminants from aquifers or from benthic sediments to surface waters [*Church*, 1996]. Groundwater seepage could influence water quality in San Francisco Bay because there are high levels of contaminants, including metals, in its benthic sediments [*Luoma and Phillips*, 1988; *Rivera-Duarte and Flegal*, 1997a, 1997b; *van Geen and Luoma*, 1999]. Therefore we determined groundwater seepage rates and bioirrigation rates in northern San Francisco Bay, and estimated the importance of benthic seepage on the transport of dissolved metals to its surface waters.

[3] A variety of methods have been employed to determine groundwater flux rates across the sediment-water interface.

0043-1397/02/2001WR000827$09.00

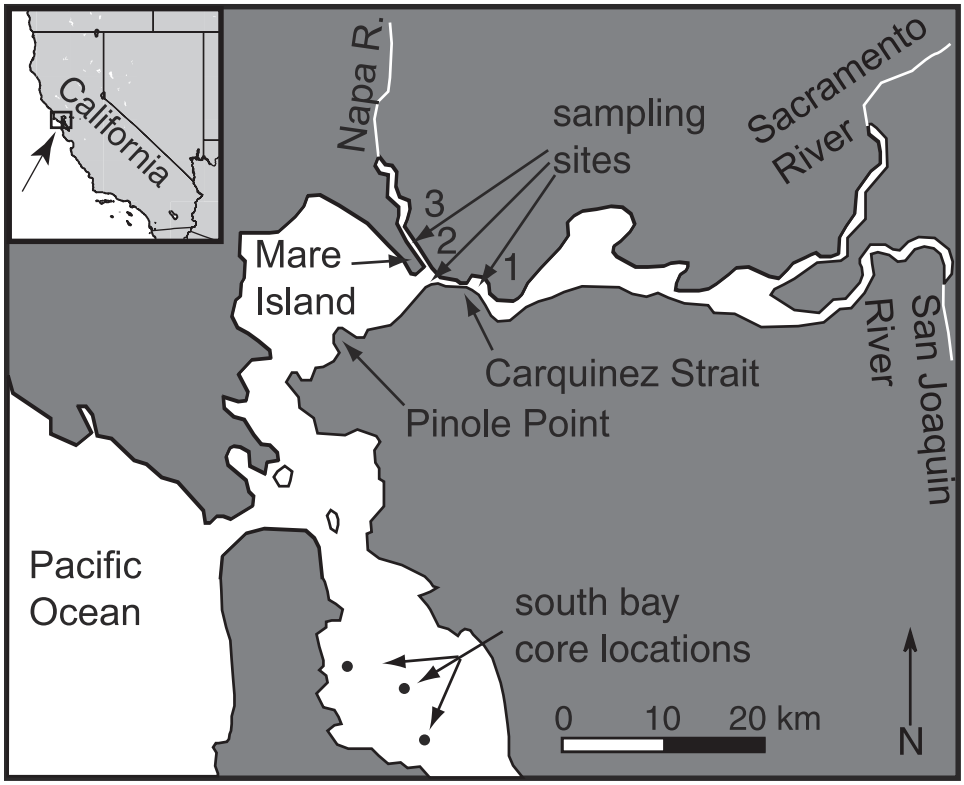

Figure 1. Map of northern San Francisco Bay with the three sampling sites in Carquinez and Mare Island Straits where we determined groundwater seepage rates and bioirrigation rates in bay floor sediment. Also shown are the locations of three southern San Francisco Bay sediment cores used for comparison to the northern bay cores.

Seepage meters have been used to determine groundwater seepage rates into lakes [*Lee*, 1977; *Fellows and Brezonik*, 1980; *Woessner and Sullivan*, 1984; *Cherkauer and Zager*, 1989], estuaries [*Gallagher et al.*, 1996; *Robinson et al.*, 1998], and coastal environments [*Giblin and Gaines*, 1990; *Cable et al.*, 1997]. Groundwater seepage rates have also been determined based on hydraulic head gradients [*Woessner and Sullivan*, 1984; *Cherkauer and Zager*, 1989; *Robinson et al.*, 1998; *Uchiyama et al.*, 2000] and by detecting tracers in surface waters [*Hussain et al.*, 1999; *Moore*, 1999]. Pore water chemistry has been used in estuarine and marine environments to determine rates of fluid flow through sediments by fitting observed pore water profiles to solutions of diffusion-advection-reaction equations [*Hammond et al.*, 1985; *Wheat and Mottl*, 1994, 2000].

[4] Quantification of benthic seepage fluxes is important because aquifers and sediments can act as sources of contaminants to surface waters [e.g., *Gallagher et al.*, 1996; *Zelewski et al.*, 2001]. This is indicated by concentration gradients of dissolved metals in sediment pore waters in estuaries [*Rivera-Duarte and Flegal*, 1997a, 1997b] and coastal zones [*Ciceri et al.*, 1992], which show that metals flux from sediments to surface waters in some settings. Benthic chamber measurements have also documented the release of dissolved metals from sediments to surface waters [*Ciceri et al.*, 1992; *Zago et al.*, 2000]. High concentrations of dissolved metals in sediment pore waters have also indicated that the advection of groundwater and the circulation of water by bioirrigation may be important in transporting metals to surface waters. Gradients of metals from aquifers onshore toward a coastal bay indicate that the transport of metals from aquifers to surface waters could be of regional importance [*Montluçon and Sañudo-Wilhelmy*, 2001]. Similarly, groundwater can transport nutrients to surface waters [*Valiela et al.*, 1990]. Benthic nutrient exchange has been studied in southern San Francisco Bay [*Hammond et al.*, 1985], but its role in northern San Francisco Bay has not be determined [*Peterson et al.*, 1985].

1.1. Setting

[5] Our study is focused in northern San Francisco Bay (Figure 1), a well-mixed estuary with large fresh water inputs from the Sacramento and San Joaquin Rivers mixing with seawater entering through the Golden Gate [*Conomos et al.*, 1985]. The bay floor sediments are underlain by relatively high permeability interbedded sandstones and shales of the Panoche Formation that crop out in the surrounding hills and dip toward the bay [*Dibblee*, 1980]. There is moderate topographic relief onshore, allowing significant hydraulic head gradients to develop between the aquifers onshore and the bay, in contrast to the extremely low topographic relief immediately surrounding southern San Francisco Bay. The strong seasonality in precipitation, almost all rain falling in a few winter months [*Conomos et al.*, 1985], should enhance groundwater seepage in the winter and spring, when hydraulic heads onshore are highest.

1.2. Dissolved Metals in San Francisco Bay

[6] Nonconservative excesses [*Officer*, 1979] of nutrients and dissolved metals in northern San Francisco Bay surface

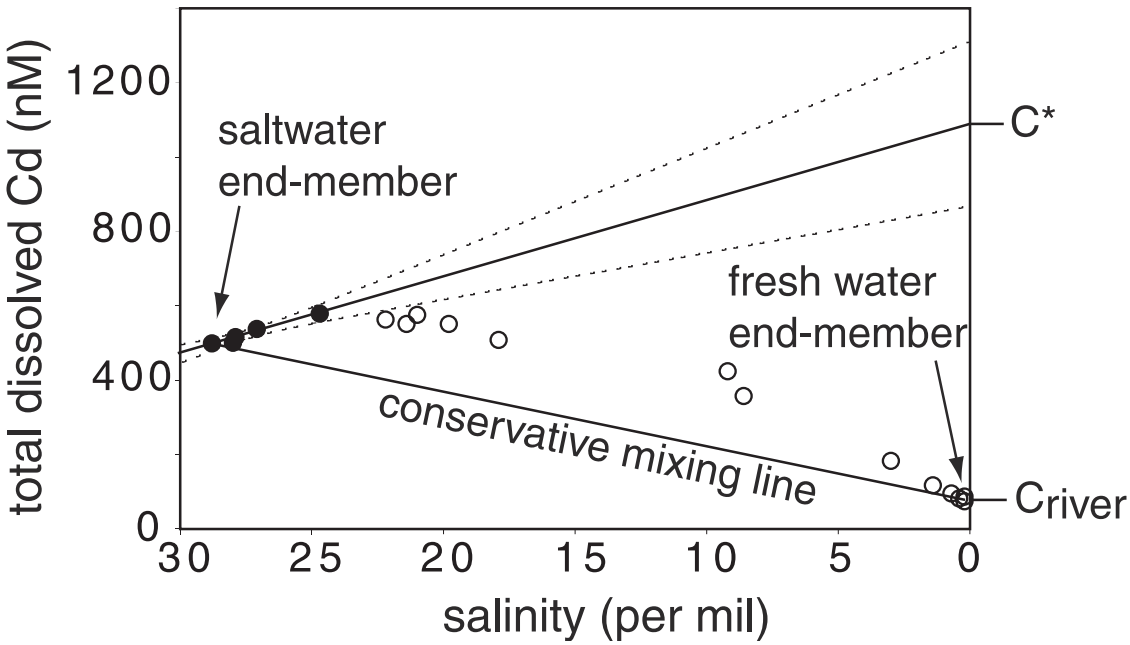

Figure 2. Concentrations of dissolved (<0.45 μm) cadmium in northern San Francisco Bay surface waters [after *Flegal et al.*, 1991]. Cadmium concentrations above the conservative mixing line indicate that there are internal sources of cadmium to the bay. The amount of cadmium added to the bay by internal sources is proportional to the difference between the cadmium concentration at the freshwater end of the system (C_{river}) and the cadmium concentration that would have to be present at the freshwater end of the system (C^*) if the oceanic end is conservative (i.e., linear). C^* is determined by fitting a straight line to the points at the oceanic end of the system (solid points) [*Officer*, 1979]. The dashed lines are 95% confidence intervals on the least squares regression.

waters [*Flegal et al.*, 1991; *Smith and Flegal*, 1993; *van Geen and Luoma*, 1999] indicate that there are sources of dissolved metals within the bay, between the Sacramento/San Joaquin Rivers and the Pacific Ocean. Preliminary mass balance calculations indicate that these internal sources are larger than known inputs to the bay [*Rivera-Duarte and Flegal*, 1997a, 1997b]. For example, in the absence of sources or sinks within the estuary, dissolved cadmium concentrations versus salinity should plot as a straight mixing line between the freshwater and saltwater end-members of this well-mixed estuary. In contrast, dissolved cadmium concentrations versus salinity in northern San Francisco Bay follow a convex-up profile, indicating that internal sources are adding dissolved cadmium to northern San Francisco Bay (Figure 2).

[7] The net internal flux of dissolved cadmium to the system is defined as:

$$F_{internal} = Q\left(C^* - C_{river}\right) \quad (1)$$

[*Officer*, 1979], where Q is the volume flux of water into the bay at the freshwater end, C^* is the dissolved cadmium concentration required at the freshwater end of the system to explain observed concentrations at the oceanic end of the system due to conservative mixing, and C_{river} is the measured concentration of dissolved cadmium at the freshwater end. Given the surface water concentrations of cadmium and the discharge from the Sacramento and San Joaquin Rivers, an average of 27 moles of dissolved cadmium are added to northern San Francisco Bay by these sources each day [*Flegal et al.*, 1991]. After accounting for estimated industrial and municipal inputs, and biological scavenging, the amount of dissolved cadmium added to northern San Francisco Bay by unknown sources is estimated to be 103 mol/d. Because particles transported into San Francisco Bay by rivers are a relatively small source of cadmium to the surface water, dissolved cadmium sources are located within San Francisco Bay [*van Geen and Luoma*, 1999]. In northern San Francisco Bay, the largest dissolved cadmium enrichments are near the Carquinez Strait (Figure 1) [*van Geen and Luoma*, 1999]. Following the same calculations as those for cadmium, similarly large, internal sources of cobalt, nickel, and copper of unknown origin also appear to be present in northern San Francisco Bay [*Flegal et al.*, 1991].

1.3. Objectives and Approach

[8] Potential sources of dissolved metals to northern San Francisco Bay that have not been well quantified include the desorption of metals from sediments which have been resuspended in the water column and the transport of dissolved metals from benthic sediments to surface waters by the advection of groundwater. Our study focuses groundwater advection. This pilot study was intended to determine the potential role of groundwater seepage in the area based on a small number of measurements, not to map local spatial variability in seepage.

[9] We used two approaches to estimate groundwater seepage rates. First, we deployed osmotic seepage meters

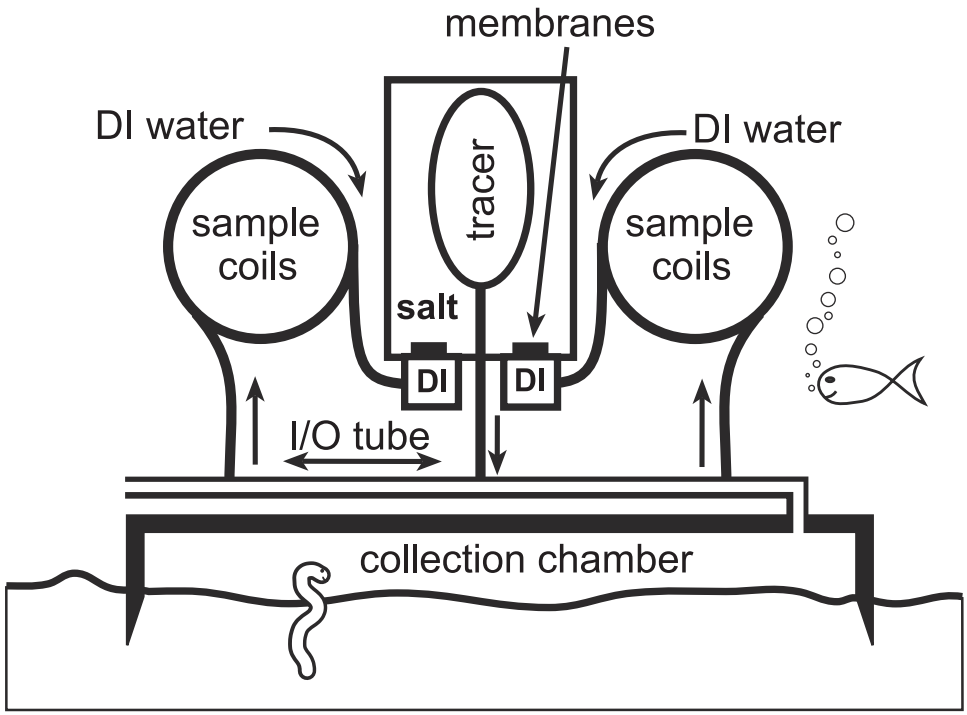

Figure 3. Schematic of osmotic seepage meter [after *Tryon et al.*, 2001]. Seepage in or out of the bay floor sediments forces water through the input/output tube. An inert tracer is injected into the I/O tube between two sample coils which draw fluid in from the I/O tube. The magnitude and direction of seepage is determined by the concentration of tracer in the two coils. Tracer injection and suction of water into the sample coils is "powered" by osmotic gradients across membranes.

[*Tryon et al.*, 2001] to measure the physical passage of fluid across the sediment-water interface. Second, we collected pore waters and analyzed them for the major ions in seawater. Concentration-depth profiles of conservative ions were compared to calculated profiles using time, diffusion, advection, and bioirrigation terms. We used the advection and bioirrigation rates estimated from these data to calculate the advective fluxes of dissolved metals across the sediment-water interface. Because we have only three sampling sites, we use a groundwater flow model [*McDonald and Harbaugh*, 1988] to characterize the pattern of offshore seepage in the Carquinez Strait. This allows us to place the seepage rates determined at our sites into context and to estimate seepage rates over larger areas of the bay floor.

2. Methods

[10] We chose three sites we thought likely to have relatively high seepage rates based on local geology (Figure 1). The sites are located in straits adjacent to highlands, in Carquinez Strait (sites 1 and 2) and in Mare Island Strait (site 3). Sediments at site 2 are coarse sand; sediments at sites 1 and 3 are dominated by silt and clay. Water depths at the sites range from 5 to 10 m, allowing for boat and SCUBA diver access. We chose sites outside of the main ship channel (~30 m water depth) for diver safety.

[11] We collected water and sediment samples and deployed instruments at each site. At site 1, we deployed pore water peepers and two osmotic seepage meters for one month, beginning in March 1999. We also collected short (~25 cm) sediment push cores in March, August, September, and November 1999, and long (~3 m) sediment cores in December 2000. Finally, we deployed an osmotic water sampler [*Wheat et al.*, 2000], which continuously collected bottom water from August to November 1999. At sites 2 and 3, we collected short sediment cores and deployed pore water peepers and osmotic seepage meters in March 1999. We retrieved the pore water peepers and seepage meters in April 1999.

[12] The pore water peepers were constructed out of polycarbonate boards with wells filled with filtered seawater and covered by a membrane [*Wheat et al.*, 1998]. The peepers were installed in the sediment for a sufficient duration for the composition of the water in the wells to equilibrate with sediment pore water chemistry. The time to reach equilibrium is a function of membrane properties, the diffusion coefficient of the ion of interest, and peeper well depth [*Webster et al.*, 1998]. Our shortest deployment was 27 days. The peepers should reach 90% equilibration is less than three days. The seepage meters and pore water peepers were installed and recovered by divers. The short sediment push cores were collected by hand by divers. The osmotic surface water sampler was secured ~1 m above the bay floor between an earth anchor in the bay floor and a polystyrene float. The long sediment cores were collected with a gravity corer using the R/V *David Johnston*.

2.1. Seepage Meters

[13] The osmotic seepage meters we deployed have been used in ocean settings on the Cascadia [*Tryon et al.*, 1999], Costa Rica [*Tryon and Brown*, 2000], and Kodiak margins [*Tryon et al.*, 2001]. They can measure benthic seepage rates from 0.1 mm yr^{-1} to 15 m yr^{-1}. Seepage flows from

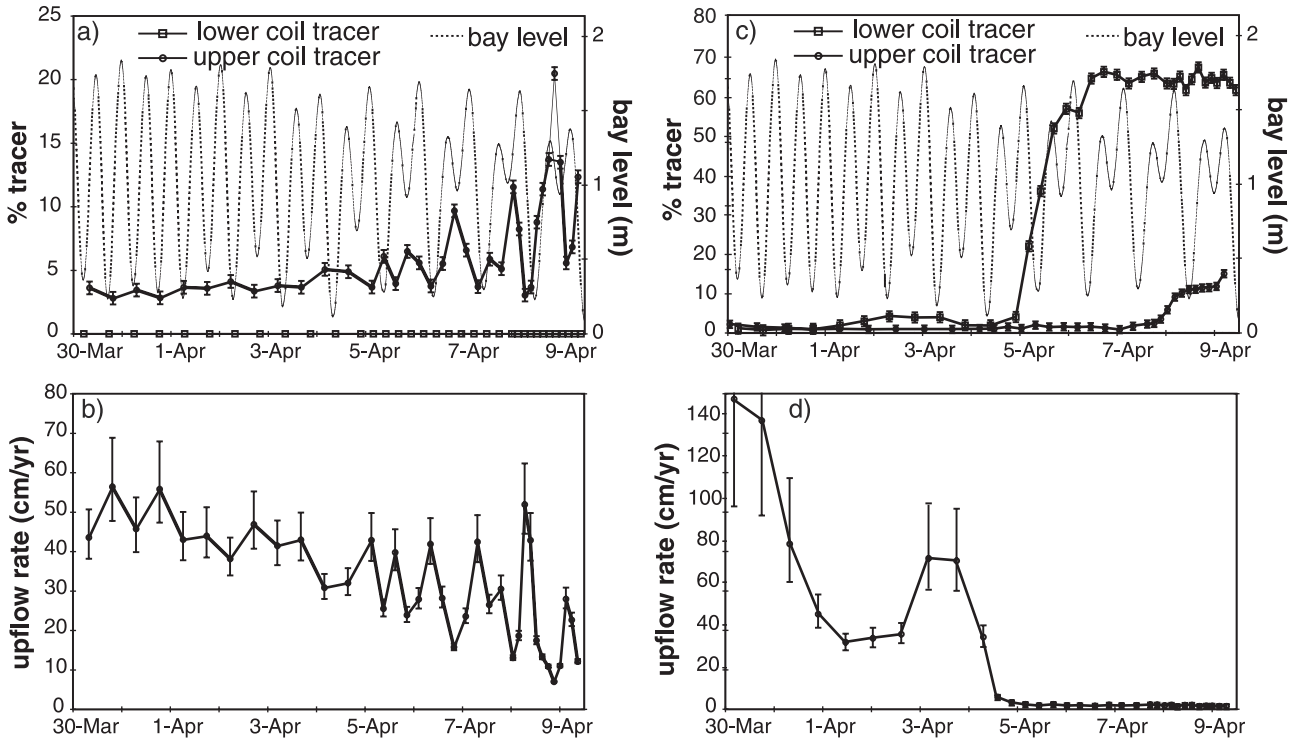

Figure 4. Results from an osmotic seepage meters deployed at sites 1 and 3 from March to April 1999. (a) The amount of tracer drawn into the upper and lower sample coils of the seepage meter at site 1 (left axis). Tracer drawn into the upper coil indicates up-directed seepage. The amount of tracer drawn into the coil is inversely proportional to the seepage rate. Height of San Francisco Bay surface water (right axis) shows tidal variations. Variable tidal behavior results from the transition from spring tides (full moon on 31 March) to neap tides (last quarter on 8 April). (b) The seepage rate determined by the seepage meter at site 1 from 30 March to 9 April 1999. The data shown are the final 10 days of a 30-day deployment, considered the most reliable data; any settling of the meter likely ceased by this time. The few samples analyzed from the earlier portion of the deployment are consistent with the 30 March to 5 April data (~4% tracer in the upper coil, no tracer in the lower coil). (c) Amount of tracer drawn into the upper and lower sample coils of the seepage meter at site 3 (left axis) and height of San Francisco Bay surface water (right axis). (d) Seepage rate determined by the seepage meter at site 3. The abrupt change in seepage rate, coincident with the changing character of tides, could indicate that the seepage meter was agitated by currents and the apparent seepage rate was altered.

the sediment through the base of the meter and through an open tube out of the chamber, ultimately into the surface water. As water flows through this inflow/outflow tube, with a velocity controlled by the seepage direction and rate, an inert tracer (0.300% RbCl in a NaCl solution) is injected into the tube. Fluid is continuously drawn into two coils of tubing, bracketing the point along the flow through tube at which the tracer is injected (Figure 3).

[14] The direction and magnitude of fluid flow through the inflow/outflow tube is determined based on the amount of tracer drawn into each of the sample coils. When the seepage meter is stationary, flow through the tube results only from seepage across the sediment-water interface. Tracer drawn into the upper coil indicates up-directed seepage. Tracer drawn into the lower coil indicates down-directed seepage.

[15] The pump that draws water into the sampling coils and injects tracer into the water is "powered" by an osmotic pressure gradient across a membrane. The sampling coils are prefilled with deionized water, and these are separated from a supersaturated salt solution by osmotic membranes. The rate of water sampling, and of tracer injection, is determined by the size and properties of the membrane, the osmotic gradient across the membrane (all of which are constant), and the temperature of the fluid. A long-term temperature logger is deployed with the meter, and corrections for sampling rate (i.e. flux rate across the osmotic membrane) as a function of temperature are made to generate a time series of tracer concentration and apparent seepage rate. Thus the osmotic seepage meter has no moving parts and no external power supply [*Tryon et al.*, 2001].

[16] For long deployments or in locations with rapid upflow, these seepage meters can also provide information about the chemical composition of groundwater seepage. If over the course of the deployment, the net volume of fluid that flows out of the sediments is sufficient to replace all of the water initially contained within the collection chamber, then the fluid drawn into the sampling coils will reflect the chemical composition of the seepage.

[17] The temporal resolution of the meter depends on the sampling rate and tubing diameter. The duration of

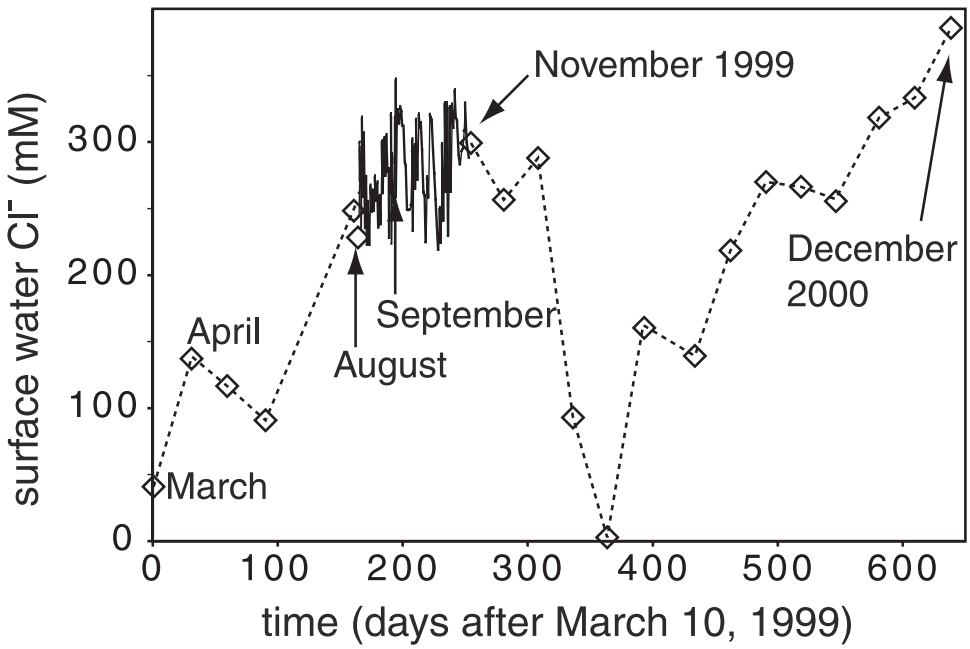

Figure 5. Chloride concentration in bottom water at site 1 from March 1999 to December 2000. The solid line, between August and November 1999, shows data from samples collected by an osmotic bottom water sampler. The diamonds show data from approximately monthly USGS water sampling.

deployment can be increased by lengthening the sampling tubing. For the purposes of this study, the deployment duration was 30 days and the highest temporal resolution was 3 hours. The meters measure flow through the inflow/outflow tube, generally interpreted to indicate seepage through the sediment-water interface. However, if the seepage meter moves vertically during deployment, for example due to settling or agitation of the meter, the fluid flow rate through the inflow/outflow tube will result from both groundwater seepage and movement of the meter.

2.2. Sediment Cores

[18] Sediment cores were collected in order to determine sediment porosity, permeability, consolidation behavior, formation factor, thermal conductivity, and the concentration of several major seawater ions in sediment pore waters. Cores for sediment physical properties measurements were collected, sealed, and stored upright at 4°C until analysis. Porosity was determined from sediment water content and grain density measurements. One-dimensional consolidation tests were performed on 1.5-cm-thick samples with a back pressured, fixed ring odometer [*Rowe and Barden*, 1966]. Vertical, permeability measurements were made using the steady state flow pump method [*Olsen et al.*, 1985] with low-gradient flows induced at multiple rates, up and down through the samples at each consolidation step. Formation factor was determined from resistivity measurements made on split cores [*McDuff and Ellis*, 1979]. Thermal conductivity was determined by the needle probe method on whole round core samples [*Von Herzen and Maxwell*, 1959]. Pore water samples were obtained immediately after core recovery by centrifuging 1-cm-thick sections of the sediment cores, extracting and filtering (0.45 μm) the water. Concentrations of chloride, magnesium, and calcium ions were determined for the pore water and surface water samples by titration. Concentrations of sodium and potassium ions were determined by ion chromatography.

3. Results

3.1. Seepage Meters

[19] A seepage meter deployed at site 1 provided an estimate of the net flux of water from the sediments to the overlying surface waters. From 30 March to 9 April 1999, tracer was drawn exclusively into the upper coil of the seepage meter (Figure 4a), indicating apparent upflow of fluid from the sediments to the surface waters. For faster updirected seepage, the tracer becomes more diluted before it can be drawn into the upper coil. Therefore, low concentrations of tracer in the upper coil correspond to high seepage rates and high concentrations of tracer in the upper coil corresponded to low seepage rates (Figure 4b). Based on those concentrations, the apparent flux rate varies from 7 to 56 cm yr^{-1}, with significant daily variations. The short period seepage amplitude oscillations are apparent where the sampling frequency is relatively high; from 5–7 April tracer concentrations are determined for samples drawn into the sampling coils approximately 6 hours apart, and from 8–9 April the sampling frequency is approximately 3 hours. Prior to 5 April, the sampling frequency is approximately 12 hours and short period variations cannot be determined. Given the physical properties of the shallow sediments at these sites, fluctuations in seepage rate due to tidally induced pore pressure variations [*Wang and Davis*, 1996] should have an amplitude on the order of 1 cm yr^{-1}, much less than the variations of up to 50 cm yr^{-1} observed in some records. These large short-term fluctuations in the apparent seepage rate may be a result of the meter moving in response to tides or currents. The average upflow rate

probably indicates the average fluid flow rate across the sediment-water interface. Another, but less likely, explanation is that the average determined seepage rate is related to the average effect of currents. The second seepage meter at site 1 failed due to a kink in the sample collection tubing.

[20] Data from the seepage meters at the other two sites provided mixed results. The seepage meters at site 2 were undermined, probably by strong currents (tidal currents of 1–3 kts are common) generating eddies and eroding sediment around the meters. Results from the seepage meter at site 3 indicate large upflow rates (>100 cm yr^{-1}) during 30–31 March, moderate upflow rates (30–80 cm yr^{-1}) during 1–4 April, and extremely low upflow rates (<2 cm yr^{-1}) during 5–9 April (Figures 4c and 4d). This abrupt change in the apparent seepage rate on 5 April is coincident with a moderate change in the character of tides.

[21] Apparent tidal pumping of fluid through the upper portions of the sediment was recorded in most of the seepage meters. Dilute tracer was drawn into both the upper and lower sampling coils of many of the meters, suggesting rapid oscillations in flow direction. In many cases this tidal flow was greater than the net flow and greatly exceeded the potential seepage rate through the sediment section due to tidally induced pore pressure variations. Such rapid reversals of flow through the meters have been observed in deep-sea cold seep environments, making it impossible to quantify the flow at a given location [*Tryon et al.*, 2001]. In our experiment this apparent tidal pumping could result from both seepage across the sediment-water interface and agitation of the seepage meters in response to tidally induced currents. As the predicted seepage due to tidally induced pore pressure variations is limited, most of the amplitude of these large oscillations likely results from agitation of the meters and bottom current induced shallow seepage (e.g., *Huettel et al.*, 1998).

3.2. Bottom Water Chemistry

[22] Seasonally variable outflow from the Sacramento and San Joaquin Rivers results in large seasonal fluctuations in the bottom water chemistry of northern San Francisco Bay [*Cloern and Nichols*, 1985]. Bottom waters in northern San Francisco Bay are generally freshest in the winter and early spring months, when river discharges are greatest. The estuary bottom waters become increasingly saline throughout the summer; maximum bottom water chloride concentrations at site 1 are approximately 70% of seawater (Figure 5).

[23] This seasonality is illustrated by bottom water chloride concentrations determined from monthly salinity measurements made by the USGS (http://www.sfbay.wr.usgs.gov/access/wqdata). Short-term temporal variations in bottom water chloride concentrations, not captured by the USGS monthly water sampling, are quantified with samples collected from mid-August to mid-November by an osmotic water sampler. Bottom water chloride concentrations are determined for 115 samples; each sample represents bottom water drawn into the sampler over ~5 hrs.

3.3. Pore Water Chemistry

[24] The pore water chemistry profiles at site 1 result from seasonal variations in the chemistry of the overlying surface waters. As a result of molecular diffusion, fluctuations in surface water chemistry will propagate into the sediment to a depth on the order of:

$$l = \sqrt{D_s t} \tag{2}$$

into the sediment, where l is the characteristic length scale, D_s is the diffusion coefficient for an ion moving through saturated sediment, and t is the period of the surface water chemistry perturbation [*Berner*, 1980]. For the diffusion of the major seawater ions in response to cyclic annual perturbations, this characteristic length scale is approximately 20 cm.

[25] Pore water chloride concentrations were relatively low in March 1999 in the shallow sediments, near the bay floor, and increased with depth to the bottom of the cores, ~20 cm. The bottom water chloride concentration increased from March to April 1999 and the chloride concentration in the pore water within the upper ~5 cm of sediment increased in response. The pore water chloride concentrations continued to increase throughout the summer and fall. Pore water from two gravity cores collected in December 2000, showed relatively small variations in chloride concentration below ~30 cm depth, indicating the depth extent of pore water response to annual perturbations (Figure 6).

4. Pore Water Modeling

[26] We used these observed seasonal variations in pore water chemistry to estimate the relative importance of diffusion, advection, and bioirrigation in transporting solutes through sediment pore waters, as defined in the following sections. We described the transport of ions through the bay floor sediments by diffusion, advection, and bioirrigation. We used a one-dimensional numerical model to find the range of advection and bioirrigation rates which provide good fits between the measured and modeled pore water chemistry in response to changing surface water chemistry.

4.1. Diffusion and Advection

[27] At any point in the sediment column, the change in ion concentration in response to diffusion and advection is described by:

$$\frac{d}{dt}(\Phi c) = \frac{d}{dz}\left(\Phi D_s \frac{dc}{dz}\right) - \frac{d}{dz}(\Phi v c) \tag{3}$$

where Φ is porosity, c is the concentration of an ion at depth, t is time, D_s is the diffusion coefficient for the ion moving through saturated sediment, z is the depth in the sediment column, and v is the average linear fluid velocity through the porous sediment [*Berner*, 1980]. The ion diffusion coefficient is defined as:

$$D_s = \frac{D_w}{\Phi F} \tag{4}$$

[*Ullman and Aller*, 1982], where D_w is the diffusion coefficient for the ion in water [*Li and Gregory*, 1974] and F is sediment formation factor. We applied porosity and formation factor measurements from one sediment core to calculations for all times; we assume they vary with depth, but not with time. We considered multicomponent diffusion, the effect that the transport of one ion has on the transport

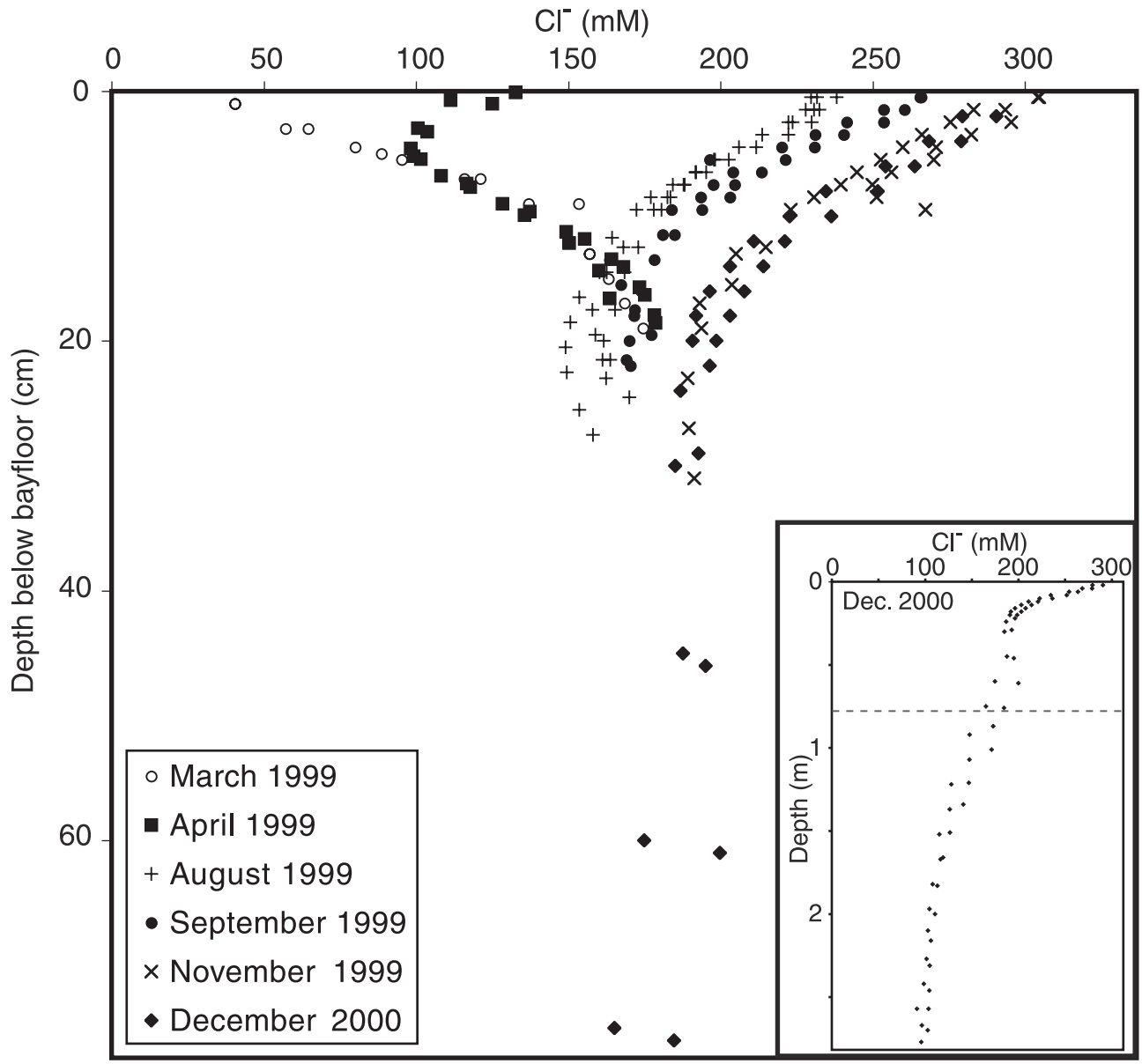

Figure 6. Chloride concentration in sediment pore water at site 1 in March, April, August, September, and November 1999 and December 2000. Seasonal surface water chemistry fluctuations (see Figure 5) propagate into the sediment. We model this transport of ions through the upper 75 cm of the sediment column in order to determine the relative importance of diffusion, advection, and bioirrigation. Chloride concentrations from the entire (~3 m long) core collected in December 2000 are shown in the inset in the lower right. Concentration gradients below 75 cm (dashed line) are relatively small and are not affected by annual variability.

rate of another in order to maintain charge balance [*McDuff and Ellis*, 1979], but this results in extremely small deviations from the single component transport case, and therefore we neglect cross diffusion coefficients in subsequent calculations.

[28] Advection of fluid through the sediment will deflect the diffusive pore water concentration profile up or down, in response to upflow or downflow, respectively (Figure 7a). The magnitude of this deflection scales with seepage rate, allowing estimation of this parameter from pore water geochemical profiles. Rapid sediment erosion or deposition would alter the pore water profiles by shifting the location of the upper boundary of the system and, in the case of deposition, incorporating bay bottom water as pore water at the top of the sediment column. Based on differencing bathymetric data, our sites have been areas of nondeposition/erosion from 1942 to 1990 [*Cappiella et al.*, 1999]. Therefore, although other portions of northern San Francisco Bay have experienced substantial sediment erosion or deposition [*Fuller et al.*, 1999; *Jaffe et al.*, 1998], our study sites are likely not affected.

4.2. Bioirrigation

[29] Bioirrigation is the exchange of surface water and pore water resulting from biological activity. In order to simulate bioirrigation, we apply a model developed from

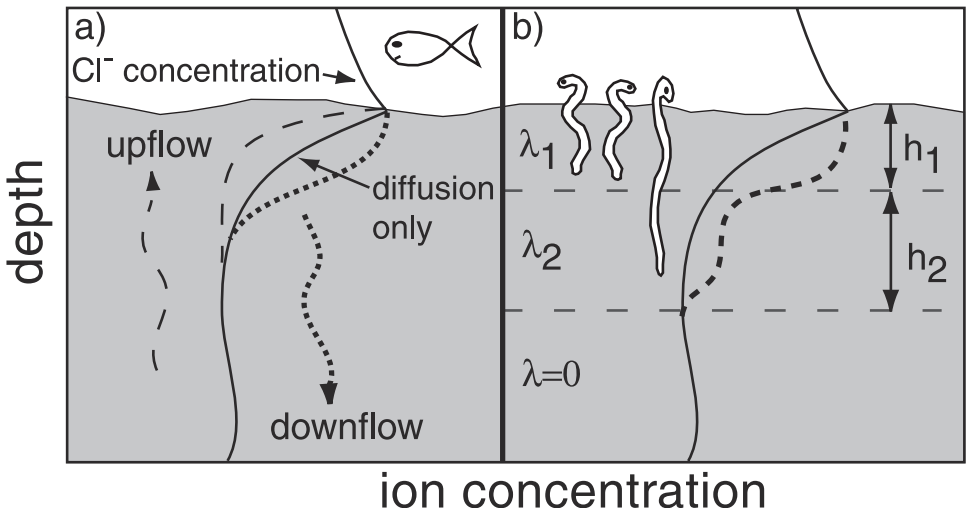

Figure 7. The effects of groundwater advection (upflow or downflow) and bioirrigation on pore water chemistry profiles. (a) Groundwater advection acts to deflect the pore water chemistry profile from the concentrations that would be present as a result of diffusion. (b) Bioirrigation replaces pore water with bottom water. We adapt a three-layered bioirrigation model [*Hammond et al.*, 1985] to our pore water modeling. Each layer is described by its thickness, h, and bioirrigation coefficient, λ, which indicates the intensity of bioirrigation.

data in southern San Francisco Bay [*Hammond et al.*, 1985]. The model represents bioirrigation with discrete layers within the sediment, each having a bioirrigation coefficient, λ [T^{-1}] (Figure 7b). We apply a three-layered model in which bioirrigation occurs only in the upper two layers. In order to reduce the number of free parameters, we use average layer thicknesses determined for south San Francisco Bay (h_1 = 15 cm, h_2 = 21 cm) and fix the relationship between the irrigation rate in the upper layer of the model, λ_1, and the irrigation rate in the middle layer,

$$\lambda_2 = 0.3\lambda_1 \tag{5}$$

based on average values for the southern reach of the estuary [*Hammond et al.*, 1985]. The change in ion concentration due to bioirrigation at any depth is described by:

$$\frac{dc}{dt} = -\lambda_i(c - c_w) \tag{6}$$

where c_w is the ion concentration in the overlying bottom water, and the subscript i indicates the bioirrigation coefficient for the appropriate layer in the sediment column. Mathematically, the bioirrigation term accounts for the exchange of pore water with bottom water, whether as a result of biological activity or other processes (e.g., surface currents [*Huettel et al.*, 1998]).

[30] Combining diffusion, advection, and bioirrigation terms yields the final equation:

$$\frac{dc}{dt} = \frac{1}{\Phi}\left[\frac{d}{dz}\left(\Phi D_s \frac{dc}{dz}\right)\right] - v\frac{dc}{dz} - \lambda_i(c - c_w). \tag{7}$$

4.3. Temperature Dependence

[31] We use a loosely coupled heat and solute transport model because the ion diffusion coefficients, D_s, are temperature dependent [*Li and Gregory*, 1974]. We model heat transport in response to conduction, advection, and bioirrigation as:

$$\frac{dT}{dt} = \kappa\frac{d^2T}{dz^2} - v\frac{dT}{dz} - \lambda_i(T - T_w) \tag{8}$$

by finite differences, in the upper 7.5 m of sediment, where T is temperature and κ is thermal diffusivity. The thermal diffusivity of sediment from site 1 is 4.5×10^{-3} cm^2 s^{-1}. The lower boundary is a constant temperature boundary, fixed at 15.5°C, the average of monthly bottom water temperature measurements at site 1 from 1989 to 1999. Temperature at the upper boundary, in the bottom water, was recorded at 5 minute intervals from 10 March to 9 April 1999 and from 20 August to 18 November 1999. The surface water temperature record was augmented with monthly bottom water measurements made near site 1 by the USGS. The distribution of temperature with depth in the sediment column is used, in combination with porosity and formation factor measurements, to calculate the diffusion coefficients for various ions at depth, which are used in the solute transport calculations.

4.4. Boundary Conditions

[32] We solve for the concentrations of several of the major ions in seawater (chloride, sodium, magnesium, calcium, and potassium) in the upper 75 cm of sediment using a finite difference approximation. The lower boundary is a constant concentration boundary, the average concentration at 75 cm, measured in December 2000 (Figure 8). We run the model over five time intervals for which we know initial and final conditions: March 1999 to April 1999, April to August, August to September, September to November 1999, and November 1999 to December 2000.

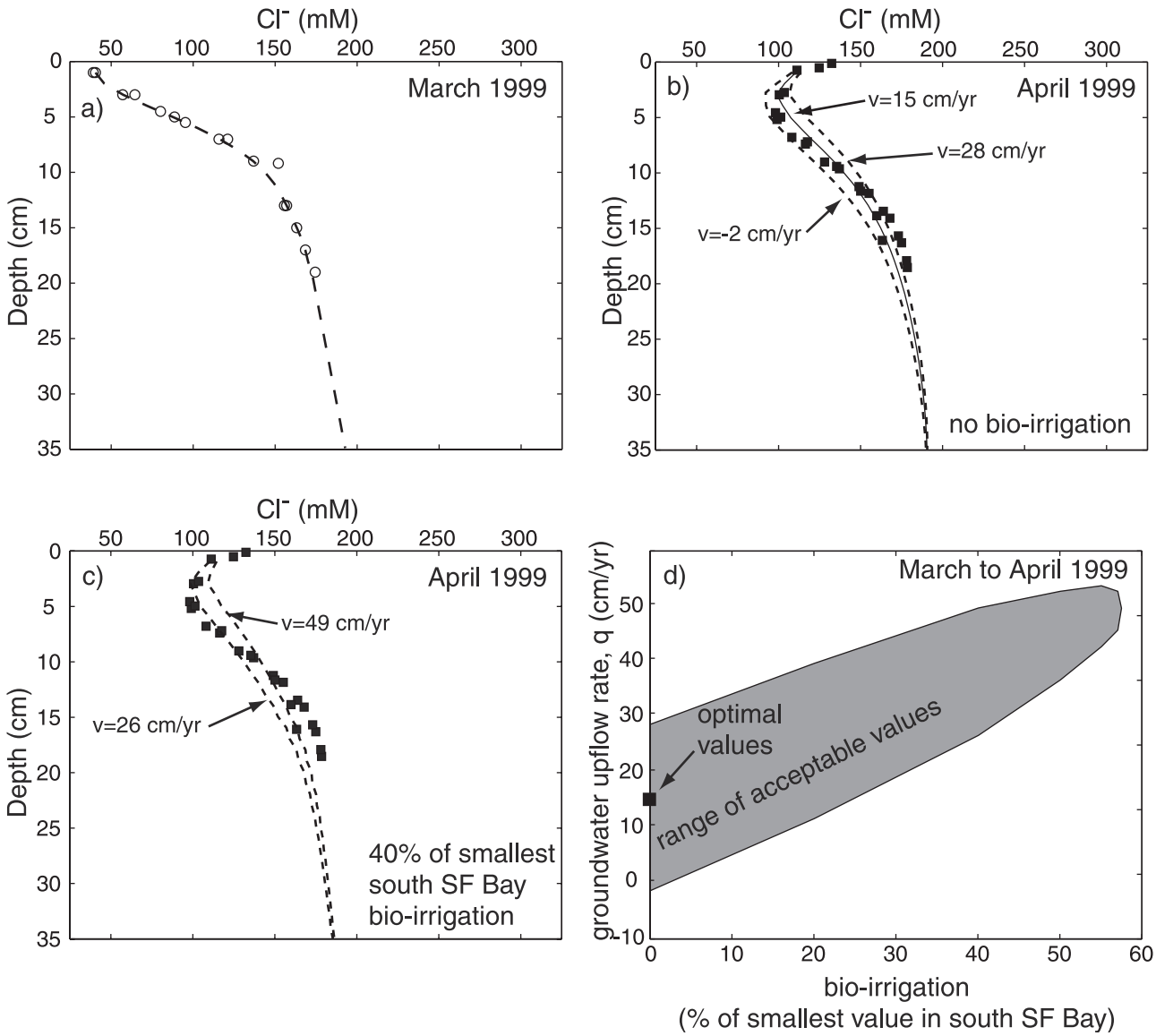

Figure 8. Results of modeling pore water chloride concentrations at site 1 from March to April 1999. (a) March pore water chloride concentrations versus depth below the bay floor. The circles show the measured pore water chloride concentrations in March. The dashed line, best fit to the measured data, is the initial condition for the chloride modeling. (b) Pore water chloride concentrations versus depth below the bay floor in April 1999. Solid squares show the measured pore water chloride concentrations. The solid line shows the model results using the optimal advection (v = 15 cm yr^{-1}) and bioirrigation rates ($\lambda_1 = 0$). The dashed lines show the model results with no bioirrigation and advection rates of −2 and 28 cm yr^{-1}, the range of upflow rates within 95% confidence limits about the optimal results. (c) Model results which fall within the 95% confidence limits of the optimal results with bioirrigation rates at 40% of the smallest rate determine in southern San Francisco Bay (see text for details). (d) The optimal advection and bioirrigation rate pair (solid circle) and the range of advection/bioirrigation rate pairs which fall within the 95% confidence limit of the optimum. Advection and bioirrigation rates are relatively small, <55 cm yr^{-1} and <60% of the smallest southern San Francisco Bay bioirrigation rate coefficient, respectively.

We use a best fit to the measured pore water concentration at the start of each time interval as the initial condition for that interval. We use a linear interpolation from the depth of the lowest pore water measurement to the lower boundary condition, and the results are relatively insensitive to reasonable modifications to this initial condition. For chloride, the upper boundary is represented by the observed surface water concentrations, a combination of ∼monthly bottom water salinity measurements and three months of continuous bottom water sampling (Figure 7). For sodium, magnesium, calcium, and potassium, the upper boundary is set with data from samples collected with the osmotic surface water sampler from August to November 1999 and from the shallowest pore water samples in March,

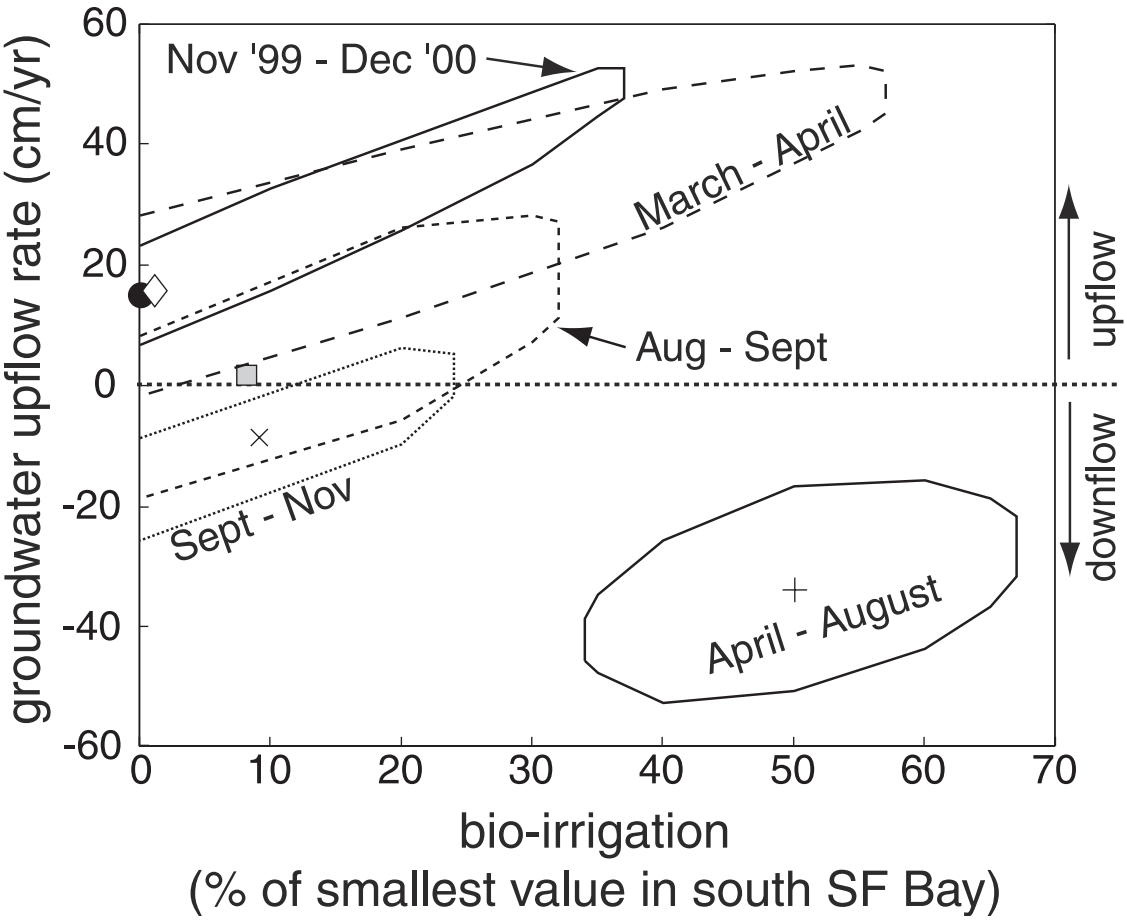

Figure 9. Ranges of advection and bioirrigation at site 1 during five sampling periods: March to April 1999, April to August, August to September, September to November 1999, and November 1999 to December 2000. Advection and bioirrigation rates are relatively small, between 55 and -55 cm yr^{-1} upflow and less than 70% of the smallest southern San Francisco Bay value, respectively.

April, August, September, November 1999, and December 2000.

5. Pore Water Model Fits to Observations

[33] Beginning with the best fit to the March 1999 chloride concentrations (Figure 8a), we change the surface water temperature and solute concentrations through time and model the solute concentrations in response to diffusion, advection, and bioirrigation. We find the combination of seepage rate and bioirrigation rate that minimizes the misfit between the model and the observations for April 1999 (Figure 8b). We use the variance of the residuals as a measure of how well we are able to simulate the observations with our model (diffusion, advection, and three layered bioirrigation). We use an F test to place 95% confidence intervals on the variance from our best fit to the observations. Then, we change the seepage rate, v, and bioirrigation rates, $\lambda_{1,2}$, to find the range of seepage and bioirrigation rates which yield variances within the 95% confidence limits. We report all bioirrigation rate results in terms of values for λ_1, since λ_2 varies linearly with λ_1 (equation 5).

[34] For example, the optimal seepage and bioirrigation rate pair to fit the chloride pore water concentrations between March and April 1999 are: upflow of 15 cm yr^{-1} and no bioirrigation. Without increasing bioirrigation, the seepage rates can range from -2 cm yr^{-1} to 28 cm yr^{-1} and the variances of the residuals still fall within the 95% confidence interval about the optimal fit to the observations (Figure 8b).

[35] The smallest bioirrigation rate coefficient determined for the upper layer of sediment in southern San Francisco Bay is $\lambda_1 = 2.4 \times 10^{-7}$ s^{-1} [*Hammond et al.*, 1985]. We report the bioirrigation rates used in our model in relation to this southern San Francisco Bay value. Increasing the bioirrigation rate from 0 to 40% of the smallest south San Francisco Bay value results in the shape of the modeled pore water chloride concentration profile fitting the observations more poorly, reducing the range of acceptable upflow rates (Figure 8c).

[36] Both the upper and lower limits on the upflow rate increase when bioirrigation is more vigorous, because bioirrigation acts to move bottom water into the sediment column, similar to down-directed seepage. The range of acceptable advection and bioirrigation rate pairs are shown in Figure 8d. Bioirrigation rates are restricted to be less than 60% of the smallest south San Francisco Bay values. Seepage (advection) rates range from -2 to 54 cm yr^{-1} depending on the bioirrigation rate that is used.

[37] We estimated ranges of advection and bioirrigation rates based on fits between modeled and observed pore water chloride concentrations from March to April 1999,

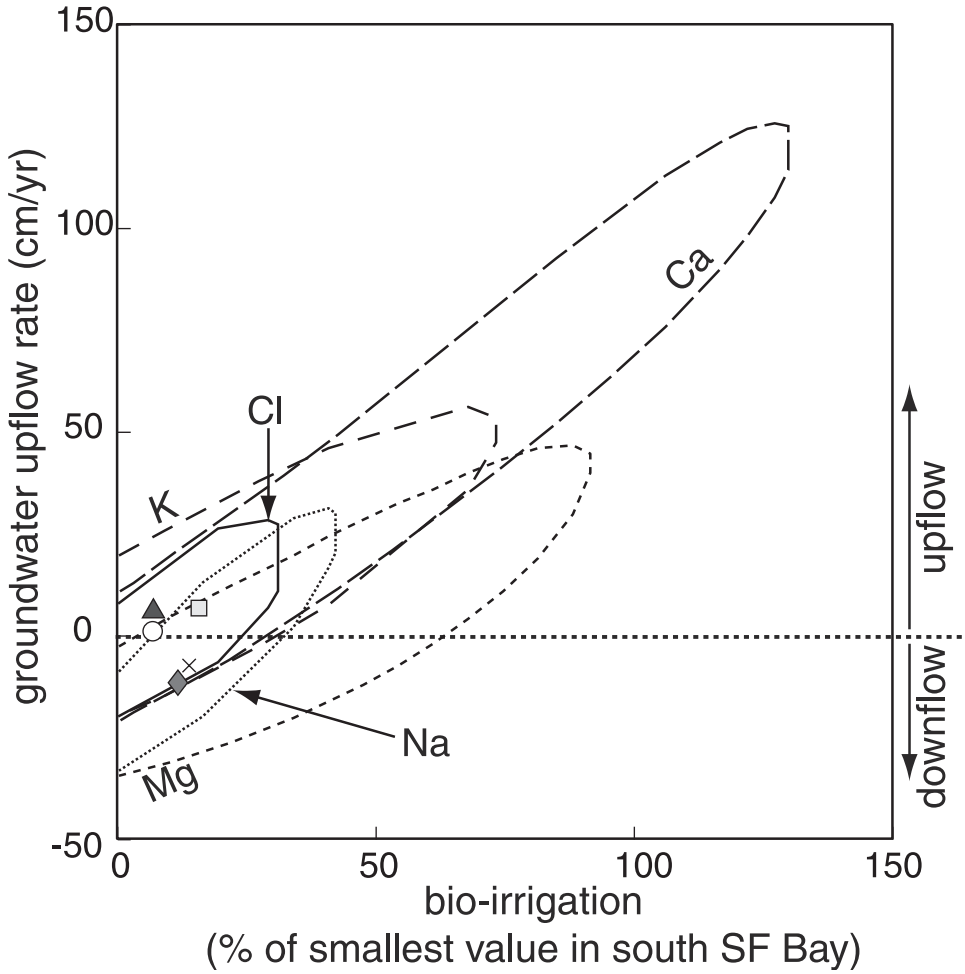

Figure 10. Comparison of advection and bioirrigation rates determined by fitting pore water concentrations of chloride, sodium, magnesium, calcium, and potassium at site 1 between August and September 1999. Advection and bioirrigation rates determined with all the ions agree. Chloride and sodium are the most conservative tracers and yield the smallest ranges of advection/bioirrigation rates. Magnesium, calcium, and potassium are more reactive, and advection/bioirrigation rates determined from their concentrations yield larger ranges.

April to August, August to September, September to November 1999, and November 1999 to December 2000 (Figure 9). Advection rates range from 55 cm yr^{-1} of upflow to 55 cm yr^{-1} of downflow depending on the bioirrigation value, which must be less than 70% of the smallest value found in south San Francisco Bay. The best fits to the measured pore water concentrations tend to be at relatively low seepage and bioirrigation rates within the ranges of possible values. Because not all of the advection and bioirrigation rate ranges outlined in Figure 9 overlap, the pore water profiles cannot be explained by a single set of advection/bioirrigation parameters.

[38] Within the northern San Francisco Bay sediment cores, macroinvertebrates were visibly sparse or absent and there was no physical evidence of bioturbation. Additionally, there are large gradients in pore water chemistry. In contrast, the upper portions of gravity cores collected at three sites in southern San Francisco Bay in December 2000 were highly bioturbated and yielded nearly vertical pore water chemistry profiles (C. G. Wheat and G. A. Spinelli, unpublished data), indicating much greater vertical mixing. The three southern San Francisco Bay cores were collected near the sites occupied by *Hammond et al.* [1985] to determine benthic fluxes (Figure 1). In northern San Francisco Bay, bioirrigation rates determined from April to August are slightly higher than in other periods (Figure 9). This is consistent with earlier results from south San Francisco Bay, suggesting that summer bioirrigation rates are slightly larger than winter rates [*Hammond et al.*, 1985].

5.1. Comparison Between Chloride and Other Tracers

[39] The advection and bioirrigation rates determined based on fits to the chloride pore water chemistry are corroborated by fits to pore water concentrations of other ions. For example, model fits to pore water chemistry between August and September 1999 show agreement between the advection and bioirrigation rates determined using chloride concentrations and the rates determined using sodium, magnesium, calcium, and potassium concentrations (Figure 10). Chloride ions are likely the most conservative tracer of fluid flow through the bay floor sediments [*Berner*, 1980]. The wider range of advection

Table 1. Advection and Bioirrigation Rates from Best Fits to Pore Water Chemistry[a]

Site	Time Period	v (cm/yr)	λ_1, % of smallest value in south San Francisco Bay
1	March–April 1999	15	0
1	April–August 1999	−34	50
1	August–September 1999	2	8
1	September–November 1999	−8	9
1	November 1999 to December 2000	16	1
2	March–April 1999	20	58
3	March–April 1999	5	0
1–3	weighted average of all results	4	13

[a] Summary of advection and bioirrigation rates determined at sites 1, 2, and 3 based on modeling chloride concentrations in sediment pore water. The average values are weighted by the length of time individual estimates cover.

and bioirrigation rates determined using magnesium, calcium, and potassium concentrations is attributed to their higher reactivity relative to chloride ions.

5.2. Comparison Between Sites

[40] Modeling the changes in pore water chloride concentration at sites 2 and 3 from March to April 1999 yield advection and bioirrigation rates similar to those found at site 1 (Table 1). The largest bioirrigation rates were determined for site 2. This relatively large value, compared to sites 1 and 3 at the same time, could be caused by a variety of chemical and physical factors, including sediment type. Sediments at site 2 are coarse sand, whereas sediments at sites 1 and 3 are dominated by silt and clay.

5.3. Temporal Variability and Comparison to Seepage Meter Results

[41] At site 1, the seepage meter results are generally consistent with advection rates estimated from pore water

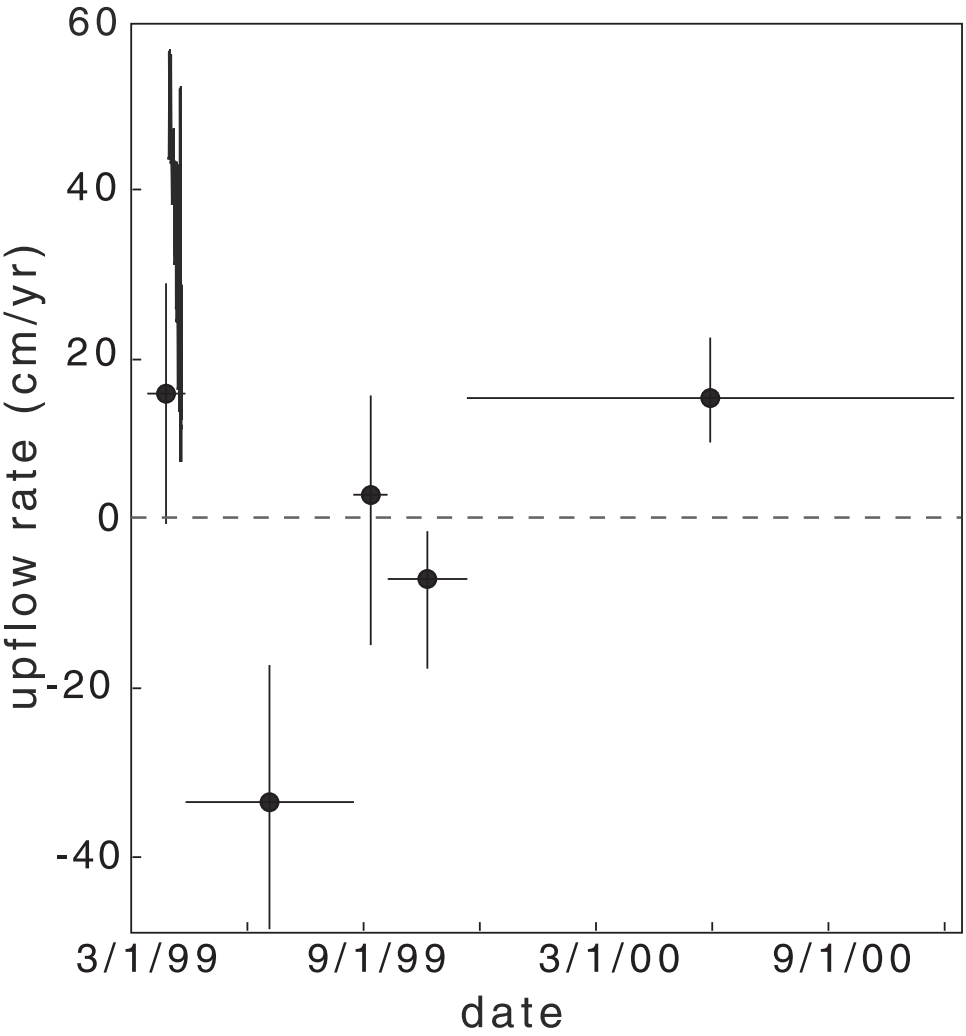

Figure 11. Summary of groundwater advection rates at site 1 from pore water chemistry and an osmotic seepage meter. The circles are optimum seepage rates determined by modeling pore water chemistry. The horizontal bars indicate the time between pore water measurements. The vertical bars indicate the 95% confidence interval on the seepage rate given the optimal bioirrigation rate (see text for details). Seepage rates determined by an osmotic seepage meter from 30 March to 9 April 1999, shown with a solid line, generally agree with the pore water chemistry results at that time.

chemistry and modeling (Figure 11). The average seepage rate through the seepage meter over this time is 36 cm yr^{-1}, compared to 15 cm yr^{-1} based on the pore water modeling. The seepage meter results (7 to 56 cm yr^{-1} upflow) span 11 days and show temporal variability, while the pore water chemistry results provide an average upflow rate for a month or more. Although 95% confidence intervals allow for ranges of advection rates of ±10 cm yr^{-1}, the confidence intervals for sequential measurements at site 1 overlap in only one of four cases, suggesting that temporal variability can be discerned from potential artifacts. Site 1 is located 600 m offshore, overlying a thick sediment column. As such, daily variations in precipitation (and presumably aquifer recharge) during the deployment of the seepage meters are unlikely to influence measured values.

[42] The seepage meters at site 2, which were undermined and tipped by strong currents, clearly demonstrate the difficulty of using this technology in a dynamic estuarine environment. At site 3, the apparently rapid seepage rates (>100 cm yr^{-1}) and perceptible sensitivity of the meter to varying tidal conditions may indicate that the seepage meter was settling into the bay floor sediments and was agitated by tides or currents. The average seepage rate at site 3 based on pore water chemistry is 5 cm yr^{-1}.

6. Groundwater Flow Model

[43] We use the advection and bioirrigation rates estimated from the pore water chemistry profiles to assess the potential importance of benthic fluxes of dissolved metals to northern San Francisco Bay. Because we have only three sampling sites, we use a groundwater flow model [*McDonald and Harbaugh*, 1988] to characterize the pattern of offshore seepage in the Carquinez Strait. This allows us to place the seepage rates determined at our sites into context and to estimate seepage rates over larger areas of the bay floor.

[44] We modeled groundwater flow along a 2-D cross section from a topographic high, ~2 km inland, across site 1 to the center of the Carquinez Strait (Figure 12a). The Panoche Formation, interbedded sandstone and shale, is exposed onshore and dips toward the bay. Within the bay, and locally adjacent to the bay, the Panoche Formation is covered by bay mud. The thickness of the bay mud increases offshore to the edge of a channel that trends down the center of the strait, then decreases to the center of the channel [*Treasher*, 1963]. Site 1 is located approximately 600 m offshore, at a water depth of ~10 m. This site, near the edge of the channel, is underlain by the thickest blanket of sediment in the area. Sites 2 and 3 are similarly located in straits, near the edges of channels.

6.1. Boundary Conditions

[45] We modeled groundwater flow in response to recharge and evapotranspiration onshore, given that the bay acts as a constant head boundary (Figure 12a). Within the model, the uppermost cells onshore cycle from 6 months of recharge to 6 months of evapotranspiration, simulating seasonal variability in precipitation. During the 6 month recharge season, the recharge rate is 400 mm yr^{-1}, assuming one third of local precipitation infiltrates and recharges the aquifer (precipitation/evapotranspiration data available at http://www.cdec.water.ca.gov). During the 6 dry months, the evapotranspiration rate is a function of the water table depth; decreasing linearly from 1600 mm yr^{-1} at the ground surface to an extinction depth of 20 m. When the depth of the water table below the ground surface exceeds the extinction depth, evapotranspiration from the water table ceases [*McDonald and Harbaugh*, 1988]. The model was run until the hydraulic heads onshore uniformly oscillated between dry season and wet season values with no interannual variability. The bay was considered a constant head boundary; the uppermost offshore cells in the model are constant head cells. The side and lower boundaries of the model are no-flow boundaries. The left boundary is a topographic, and assumed hydrogeologic, divide. The right boundary, the center of the bay, is underlain by the Rodgers Creek fault [*Dibblee*, 1980], a potential hydrogeologic boundary. The center of the bay would also be a no-flow boundary based on symmetry, assuming groundwater flows from aquifers on both shores toward the bay. The bottom of the model was set to a depth of 300 m below the bay surface and is a no-flow boundary. We used a hydraulic conductivity for the Panoche Formation of 0.31 m d^{-1}, determined from a slug test in a well completed in fractured Panoche Formation on Mare Island [*Department of the Navy*, 1998]. For the bay mud overlying the Panoche Formation, we calculated the effective vertical hydraulic conductivity as a function of sediment thickness. We measured both how the sediment porosity decreases with increasing effective stress (during consolidation tests) and how the sediment permeability changed with decreasing porosity for three samples from site 1. We approximated the sediment as a layered system and determine permeability versus depth in the sediments, given our knowledge of permeability as a function of effective stress. Then, we determined the effective vertical hydraulic conductivities of variably thick sediment columns using a harmonic mean rule.

6.2. Results

[46] In our groundwater flow simulations, the seepage rate decreases offshore to the edge of the channel at the center of the strait, then increases as the sediment cover thins (Figure 12b). This is consistent with previous demonstrations that the rate of benthic groundwater seepage is controlled largely by the distance from the shoreline and sediment thickness [e.g., *Genereux and Bandopadhyay*, 2001]. Varying the hydraulic conductivity of the underlying Panoche Formation or the recharge or evapotranspiration rates alters the absolute rates of groundwater seepage, but not its offshore distribution.

[47] As our interest is in placing our point measurements of seepage rates into a broader context, we normalize the modeled seepage distribution to the maximum seepage value. The normalized seepage rates indicate that upflow 600 m offshore, at site 1, is approximately 25% of the maximum upflow rate and approximately 45% of the average upflow rate (Figure 12b).

7. Dissolved Metals Input to Bay

[48] Using pore water chemistry profiles of dissolved metals (Co, Ni, Cu, Zn, Cd, and Ag) in northern San Francisco Bay sediments in combination with our seepage and modeling results, we estimate the flux of dissolved metals from sediments to surface waters. We treat these

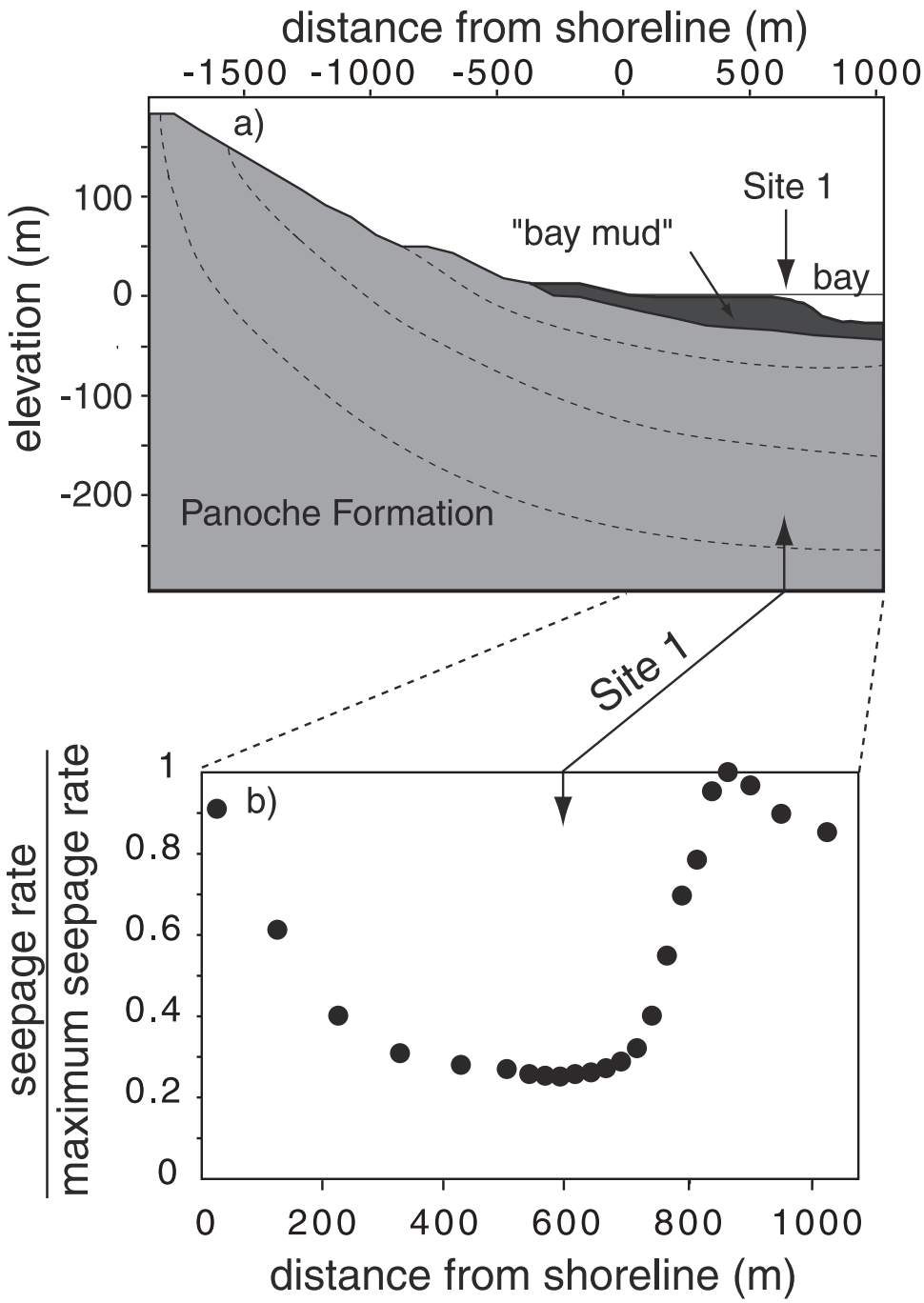

Figure 12. (a) Schematic of the geology modeled in the groundwater flow simulation. Interbedded sands and shales of the Panoche Formation (bedding shown with dashed lines) crop out in the hills surrounding the bay and dip under the bay. Bay mud covers the bay floor, thickest at the edge of the channel trending down the course of the bay. (b) Results of groundwater flow modeling, normalized seepage rate from the shoreline to the center of the bay. The seepage rate at site 1, ~600 m offshore, is approximately 25% of the maximum seepage rate and approximately 45% of the average seepage rate.

dissolved metals as conservative tracers. Actual metals fluxes could be smaller due to many factors including scavenging, bioutilization, and changes in redox state. At low seepage rates, removal processes could strip these metals from solution resulting in no advective flux to the bay waters, as demonstrated for manganese by *Wheat and McDuff* [1995]. Below we estimate metal fluxes resulting from the various transport mechanisms (diffusion, advection, and bioirrigation) to address the potential impact of groundwater seepage into the bay.

[49] We use the pore water dissolved metal concentrations determined offshore Pinole Point, the closest dissolved metals data to our sampling sites (Figure 1). The metal concentrations in pore waters offshore Pinole Point are generally comparable to four other locations in northern and central San Francisco Bay (three in Castro Cove and

Table 2. Benthic Fluxes of Dissolved Metals in Northern San Francisco Bay[a]

Element	$F_{diffusive}$, mol/d	$F_{advective}$, mol/d	$F_{bioirrigation}$,[b] mol/d)	Unknown Sources, mol/d	Unknown Sources Minus Benthic Fluxes, mol/d	Percentage of Unknown Sources Accounted for by Benthic Fluxes, mol/d
Cadmium	−0.3	0.0	−0.1	100	100	0
Cobalt	33	6	2	120	79	35
Copper	−6	1	−4	730	739	−1
Nickel	11	4	−1	1100	1086	1
Silver	0.0	0.0	0.0	0.5	0.5	0
Zinc	56	9	4	−460	−529	−15

[a] Preliminary estimates of benthic fluxes (diffusive, advective, and bioirrigation) of dissolved metals to northern San Francisco Bay surface waters. These estimates indicate that benthic fluxes of metals account for a small fraction of the unknown sources of dissolved metals to northern San Francisco Bay.
[b] For these calculations, $h_1 = 15$ cm; $h_2 = 21$ cm; $\lambda_1 = 3.1 \times 10^{-8}$ s^{-1}; $\lambda_2 = 0.94 \times 10^{-8}$ s^{-1}.

one in Oakland Harbor) [*Rivera-Duarte and Flegal*, 1997b]. The diffusive flux of dissolved metals to northern San Francisco Bay surface waters was previously estimated by *Rivera-Duarte and Flegal* [1997a, 1997b]. They calculated the diffusive flux per unit area, based on the concentration gradient between the surface water and the pore water 1 cm below the bay floor, and assumed a constant diffusive flux over the shallow portions of northern San Francisco Bay (164×10^6 m^2). We apply the diffusive flux of dissolved metals per unit area, determined from their pore water and surface water concentrations,

$$F_{diffusive} = -\Phi D_s \frac{dc}{dz} \tag{9}$$

over the entire area of northern San Francisco Bay (263×10^6 m^2).

[50] In order to estimate the advective flux of dissolved metals, we determine an average upflow rate from our three sites (Table 1). This is the average of the upflow rates that best fit observations of pore water profiles, weighted by the number of months over which each upflow rate was determined. This average upflow rate is assumed to represent 45% of the regional average upflow rate, based on results of groundwater modeling. The resulting regional average upflow rate is 10 cm yr^{-1}. Excluding removal processes, the advective flux of dissolved metals per unit area is:

$$F_{advective} = qc_{0cm} = v\Phi c_{0cm} \tag{10}$$

where q is specific discharge and c_{0cm} is the dissolved metal concentration at the sediment-water interface. We use the dissolved metal concentration one cm below the bay floor to approximate the concentration at the sediment-water interface. There are few burrows or macrofauna present in the sediments at our sampling sites. Advective fluid flow through these sediments is likely diffuse; it is not focused in burrows, in which case a metal concentration representative of the bioturbated zone may be more appropriate [*Aller*, 1984]. Using dissolved metal concentrations in pore water one cm below the bay floor in this calculation could lead to overestimates of advective dissolved metal fluxes if pore waters at the sediment-water interface are substantially more oxic and have lower dissolved metals concentrations. For this and previously stated reasons, actual advective metal fluxes could be smaller than our estimates.

[51] The bioirrigation flux is determined by applying the average estimated bioirrigation rates from our three sites to the dissolved metal pore water data. The bioirrigation flux per unit area is described by:

$$F_{bio-irrigation} = [h_1\lambda_1(c_1 - c_w)] + [h_2\lambda_2(c_2 - c_w)] \tag{11}$$

where c_1 and c_2 are the average dissolved metal concentrations in layers 1 and 2 of the bioirrigation model, respectively, and c_w is the concentration of dissolved metal in the bottom water. The bioirrigation flux is the flux resulting from the exchange of bottom water and pore water. Therefore, it is a function of the dissolved metal concentration of the pore water relative to the bottom water.

[52] Estimated dissolved metals fluxes resulting from diffusion, advection, and bioirrigation applied over northern San Francisco Bay are shown in Table 2. The benthic fluxes of most dissolved metals (Ag, Cd, Cu, Ni, Zn) represent relatively small percentages ($\leq$2%) of the unknown sources. The estimated benthic fluxes of cobalt account for ~35% of the unknown sources. Even applying the highest upflow and bioirrigation rates allowed by the pore water modeling (weighted averages of maximum values from each period), 68 cm/yr and 43% of the smallest south San Francisco Bay bioirrigation coefficient, respectively, benthic fluxes account for less than 4% of the unknown sources of all metals except cobalt. For cobalt, these extreme values allow seepage to account for ~60% of the unknown sources.

[53] The relatively high benthic flux of cobalt predicted by this simple model is a result of relatively high concentrations of dissolved cobalt in pore waters from shallow sediments. The high concentrations of dissovled cobalt in shallow San Francisco Bay sediment pore waters is consistent with other analyses of cobalt both within the bay and elsewhere. Previous mass balance calculations based on dissolved cobalt concentrations in surface waters in the bay indicated that cobalt was extensively (>99%) scavenged onto suspended particulates and subsequently remobilized from those sediments [*Flegal et al.*, 1991]. Similar internal cycling was observed in the estuarine waters of Galveston Bay [*Wen et al.*, 1999]. That internal cycling, as well as the cycling of cobalt in coastal and ocean waters, is attributed to the very high covariance of cobalt with manganese in redox processes [*Kanuer et al.*, 1982; *Martin and Gordon*, 1988; *Sañudo-Wilhelmy and Flegal*, 1996; *Sañudo-Wilhelmy et al.*, 2002]. In addition, the affinity of cobalt for organic colloids is relatively low (~20%) in estuarine waters [*Wen*

et al., 1999]. Consequently, early diagenetic processes release relatively large amounts of highly labile cobalt in near surface sediments, where it can readily migrate back into overlying waters.

[54] Several factors could contribute to greater advective transport of metals from benthic seepage to northern San Francisco Bay. These include (1) mean seepage rates considerably greater than those estimated in this study, (2) sediment metal concentrations and availability for transport that are significantly greater, or (3) local seepage rates that are significantly greater. Our determination that advective transport is relatively limited is based on several important characteristics of the way in which these calculations have been made. First, the sites we selected are thought to be favorable for seepage based on local geology. This contrasts with the geology at many other areas within northern San Francisco Bay, which are not located immediately adjacent to exposed, topographically abrupt, sandstone outcrops that dip steeply into the bay. Based on the size of the study area and on observational and modeling results, the seepage mass flux would need to be 30 times greater than that estimated to account for currently measured concentrations of cadmium, copper, nickel, silver, and zinc. Second, the metal concentrations used in this analysis are representative of several sites in northern and central San Francisco Bay [*Rivera-Duarte and Flegal*, 1997b]. If average pore water metals concentrations are actually greater than observed at these sites, advective fluxes could be greater. Given the estimated groundwater seepage and bioirrigation rates, in order for benthic fluxes to account for all the unknown sources of dissolved metals, the average concentration of dissolved cobalt in pore water 1 cm below the bay floor would have to be approximately 100 times greater than that measured offshore Pinole Point by *Rivera-Duarte and Flegal* [1997b]. Similarly, average copper, nickel, and silver concentrations 1 cm below the bay floor would have be to 1000 times greater and cadmium concentrations would have to be 100,000 times greater than measured offshore Pinole Point. Dissolved metal concentrations this high have not been reported for San Francisco Bay pore waters. Our analyses ignored variations in redox conditions within bay floor sediments and bay waters. Since trace metals are generally more mobile in reduced, rather than oxidized forms [*Sundby et al.*, 1986], the movement of metals across a redox boundary within shallow bay floor sediments is likely to reduce their rate of advection along with seepage fluids, yielding net fluxes lower than those estimated (Table 2). If there were areas where groundwater discharge was focused and seepage rates were significantly greater, the concentrations of metals in the sediments within these smaller areas would need to be commensurately greater in order to account for the necessary mass flux. Even if elevated metals concentrations were coincidentally colocated with areas of rapid local seepage, advective transfer from sediments to the bay would, presumably, rapidly deplete these sources.

[55] It is possible that there are areas of more focused groundwater discharge than we observed, and that elevated metals concentrations in these areas are sustained by lateral flow within the sediments or a more deeply seated source of dissolved metals. In fact, there is visual evidence for the intrusion of groundwater along the bank where shimmering water has been observed and freshwater growing plants survive. While the seepage rates and estimated metals fluxes from our three sites suggest that diffuse seepage throughout northern San Francisco Bay is not major source for most metals, focused discharge at other sites could be important to metals budgets. While the seepage rates and estimated metals fluxes from our three sites suggest that diffuse seepage throughout northern San Francisco Bay is not major source for most metals, focused discharge at other sites could be important locally. Another potentially important source of dissolved metals to northern San Francisco Bay surface water is the resuspension of sediments with metals adsorbed on them. Once in the water column, the metals may more easily desorb from the sediments. This has been demonstrated with laboratory experiments with sediments from south San Francisco Bay which show rapid desorption of Cu and Zn from resuspended sediment [*Gee and Bruland*, 1999, 2002]. Those desorption studies are consistent with analyses of water samples from the North Sea, which indicate that the resuspension of sediment provides a source of both particulate and dissolved metals to surface waters [*Millward et al.*, 1998]. Similarly, data from sediment traps in Lake Houston, Texas evidence the desorption of trace elements from resuspended sediment occurs [*Matty et al.*, 1987].

8. Summary and Conclusions

[56] We use seepage meters and modeling of seasonal variations in pore water chemistry to estimate rates of groundwater seepage and bioirrigation through bay floor sediments at three sites in northern San Francisco Bay. Groundwater seepage rates are within a range from upflow of 55 cm yr^{-1} to downflow of 55 cm yr^{-1}. Seepage rates that are most consistent with pore water data range between upflow of 20 cm yr^{-1} and downflow of 34 cm yr^{-1}, with an average of 4 cm yr^{-1} upflow. Groundwater flow modeling indicates that the seepage rates at these sites likely represent minimum seepage rates in the area, $\sim$25% of maximum rates and $\sim$45% of average rates. Bioirrigation rates in northern San Francisco Bay appears to be less than 85% of the smallest values estimated for southern San Francisco Bay.

[57] The results from the seepage meters and pore water chemistry are generally consistent. The seepage meters detect small changes in seepage amplitude and provide fine temporal resolution (highest resolution in this study was approximately 3 hours per sample). However, the seepage meter data is more variable due to difficulties deploying this technology in the energetic estuarine setting of northern San Francisco Bay. The pore water chemistry provides more robust, time averaged, advection rates. Also, modeling pore water chemistry provides separate estimates of advection and bioirrigation rates; the seepage meters measure the net fluid flux across the sediment-water interface, incorporating both mechanisms.

[58] The apparent difference in the degree of bioirrigation between different regions of San Francisco Bay suggests that it may not be appropriate to apply irrigation rates determined in southern San Francisco Bay to northern San Francisco Bay, or visa versa. The highest bioirrigation rate value estimated at our northern San Francisco Bay sites

occurred at a site with coarse sediment and strong currents (site 2). The relatively high "bioirrigation" rate at this site may be a result of strong currents impinging on a permeable bed [*Huettel et al.*, 1998]. However, pore water chemistry of conservative tracers requires little exchange of fluid across the sediment-water interface at these sites, whether that flow in our model is parameterized as bioirrigation or the impact of surface currents.

[59] In marine environments, where variations in surface water chemistry are generally small, pore water chemistry can detect the flow of water through sediments with velocities on the order of 0.001 mm yr^{-1} [*Ingebritsen and Sanford*, 1998]. In this estuarine environment, where surface water chemistry varies widely, both temporally and spatially, the range of advection rates over which modeling pore water chemistry is a useful tool is shifted toward much higher velocities. Consequently, seepage rates of centimeters to tens of centimeters per year ($\sim$4 orders of magnitude larger than in marine environments) are required in order to produce measurable variations in pore water chemistry in San Francisco Bay.

[60] We estimate the importance of benthic sources of dissolved metals to surface waters by applying average groundwater seepage and bioirrigation rates to pore water dissolved metals concentrations. We find that, for this set of environmental conditions, the transport of dissolved metals from sediments to northern San Francisco Bay surface waters by diffusion, advection, and bioirrigation accounts for less than 4% of the unknown sources of dissolved silver, cadmium, copper, nickel, and zinc, and less than 60% of the unknown sources of dissolved cobalt. These metal flux estimates treat dissolved metals as conservative tracers and, therefore, should be considered maximum values. Thus the source of excess metals is not likely slow seepage such as that found at these sites, but could result from more focused flow or an entirely different mechanism, such as sediment resuspension.

[61] **Acknowledgments.** We gratefully acknowledge the assistance of Don Canestro and Peter DelFarro who dove under difficult conditions to deploy and recover instruments and collect samples. Josh Plant assisted with chemical analyses. Jay Christofferson and John Keever of the California Maritime Academy kindly allowed us to stage sampling and instrumentation operations in the CMA boathouse, and "Gep" Gephart provided local assistance. We would also like to thank Gordon Smith (captain of R/V *David Johnston*), Kevin O'Toole, Walt Olson, Tim Elfers, Kit Conaway, Kim Bracchi, and Jennifer Ostrowski for field assistance. This research was supported by project SC98-59 of the U.C. Toxic Substances Research and Teaching Program and the Monterey Bay Regional Studies program at UC Santa Cruz, NSF Graduate Research Training grant (GER-9553614) in Multidisciplinary Regional Studies to Laurel Fox and Margaret FitzSimmons. This manuscript was improved by the comments of two anonymous reviewers.

References

Aller, R. C., The importance of relict burrow structures and burrow irrigation in controlling sedimentary solute distributions, *Geochim. Cosmochim. Acta*, *48*, 1929–1934, 1984.

Berner, R. A., *Early Diagenesis: A Theoretical Approach*, Princeton Univ. Press, Princeton, N. J., 1980.

Cable, J. E., W. C. Burnett, and J. P. Chanton, Magnitude and variations of groundwater seepage along a Florida marine shoreline, *Biogeochemistry*, *38*, 189–205, 1997.

Cappiella, K., C. Malzone, R. Smith, and B. Jaffe, Sedimentation and bathymetry changes in Suisun Bay: 1867–1990, *U.S. Geol. Surv. Open File Rep.*, *99–563*, 1999.

Cherkauer, D. S., and J. P. Zager, Groundwater interactions with a kettle-hole lake: Relation of observations to digital simulations, *J. Hydrol.*, *109*, 167–184, 1989.

Church, T. M., An underground route for the water cycle, *Nature*, *380*, 579–580, 1996.

Ciceri, G., S. Maran, W. Martinotti, and G. Queirazza, Geochemical cycling of heavy metals in a marine coastal area: Benthic flux determination from pore water profiles and in situ measurements using benthic chambers, *Hydrobiologia*, *235/236*, 501–517, 1992.

Cloern, J. E., and F. H. Nichols, Time scales and mechanisms of estuarine variability, a synthesis from studies of San Francisco Bay, *Hydrobiologia*, *129*, 229–237, 1985.

Conomos, T. J., R. E. Smith, and J. W. Gartner, Environmental setting of San Francisco Bay, *Hydrobiologia*, *129*, 1–12, 1985.

Department of the Navy, Groundwater Status Report: A summary of groundwater monitoring from November 1992 to May 1994, Sports Environmental Detachment, Mare Island Naval Shipyard, Vallejo, Calif., 1998.

Dibblee, T. W., Jr., Preliminary geologic map of the Benicia Quadrangle, Contra Costa and Solano Counties, California, *U.S. Geol. Surv. Open File Rep., 81-234*, 1980.

Fellows, C. R., and P. L. Brezonik, Seepage flow into Florida lakes, *Water Resour. Bull.*, *16*(4), 635–641, 1980.

Flegal, A. R., G. J. Smith, G. A. Gill, S. Sanudo-Wilhelmy, and L. C. D. Anderson, Dissolved trace element cycles in the San Francisco Bay estuary, *Mar. Chem.*, *36*, 329–363, 1991.

Fuller, C. C., A. van Geen, M. Baskaran, and R. Anima, Sediment chronology in San Francisco Bay, California, defined by ^{210}Pb, ^{234}Th, ^{137}Cs, and ^{239,240}Pu, *Mar. Chem.*, *64*, 7–27, 1999.

Gallagher, D. L., A. M. Dietrich, W. G. Reay, M. C. Hayes, and G. M. Simmons Jr., Ground water discharge of agricultural pesticides and nutrients to estuarine surface water, *Ground Water Monit. Rem.*, *16*(1), 118–129, 1996.

Gee, A. K., and K. W. Bruland, The novel use of stable isotopes and ICPMS to trace adsorption/desorption equilibrium and kinetic partitioning of Ni, Cu and Zn with natural particles from South San Francisco Bay, CA (abstract), *Eos Trans.*, *80*(46), Fall Meet. Suppl., F478–F479,1999.

Gee, A. K., and K. W. Bruland, Tracing Cu, Ni and Zn kinetics and equilibrium partitioning between dissolved and particulate phases in South San Francisco Bay, CA, using stable isotopes and HR-ICPMS, *Geochim. Cosmochim. Acta*, in press, 2002.

Genereux, D., and I. Bandopadhyay, Numerical investigation of lake bed seepage patterns: Effects of porous medium and lake properties, *J. Hydrol.*, *241*, 286–303, 2001.

Giblin, A. E., and A. G. Gaines, Nitrogen inputs to a marine embayment: The importance of groundwater, *Biogeochemistry*, *10*, 309–328, 1990.

Hammond, D. E., C. Fuller, D. Harmon, B. Hartman, M. Korosec, L. G. Miller, R. Rea, S. Warren, W. Berelson, and S. W. Hager, Benthic fluxes in San Francisco Bay, *Hydrobiologia*, *129*, 69–90, 1985.

Huettel, M., W. Ziebis, S. Forster, and G. W. Luther, Advective transport affecting metal and nutrient distributions and interfacial fluxes in permeable sediments, *Geochim. Cosmochim. Acta*, *62*, 613–631, 1998.

Hussain, N., T. M. Church, and G. Kim, Use of ^{222}Rn and ^{226}Ra to trace groundwater discharge into the Chesapeake Bay, *Mar. Chem.*, *65*, 127–134, 1999.

Ingebritsen, S. E., and W. E. Sanford, *Groundwater in Geologic Processes*, 341 pp., Cambridge Univ. Press, New York, 1998.

Jaffe, B. E., R. E. Smith, and L. Zink, Sedimentation and bathymetry changes in San Pablo Bay: 1856–1983, *U.S. Geol. Surv. Open File Rep., 98–759*, 1998.

Kanuer, G. A., J. H. Matin, and R. M. Gordon, Cobalt in north-east Pacific waters, *Nature*, *297*, 49–51, 1982.

Lee, D. R., A device for measuring seepage flux in lakes and estuaries, *Limnol. Oceanogr.*, *22*(1), 140–147, 1977.

Li, Y.-H., and S. Gregory, Diffusion of ions in sea water and in deep-sea sediments, *Geochim. Cosmochim. Acta*, *38*, 703–714, 1974.

Luoma, S. N., and D. J. H. Phillips, Distribution, variability, and impacts of trace elements in San Francisco Bay, *Mar. Pollut. Bull.*, *19*(2), 413–425, 1988.

Martin, J. H., and R. M. Gordon, Northeast Pacific iron distributions in relation to phytoplankton productivity, *Deep Sea Res.*, *35*, 177–196, 1988.

Matty, J. M., J. B. Anderson, and R. B. Dunbar, Suspended sediment transport, sedimentation, and resuspension in Lake Houston, Texas: Implications for water quality, *Environ. Geol. Water Sci.*, *10*(3), 175–186, 1987.

McDonald, M. G., and A. W. Harbaugh, A modular three-dimensional finite difference ground water flow model, *U.S. Geol. Surv. Tech. Water Resour. Invest. book 6*, 1988.

McDuff, R. E., and R. A. Ellis, Determining diffusion coefficients in marine sediments: A laboratory study of the validity of resistivity techniques, *Am. J. Sci.*, *279*, 666–675, 1979.

Millward, G. E., A. W. Morris, and A. D. Tappin, Trace metals at two sites in the southern North Sea: Results from a sediment resuspension study, *Continental Shelf Res.*, *18*, 1381–1400, 1998.

Montluçon, D., and S. A. Sañudo-Wilhelmy, Influence of net groundwater discharge on the chemical composition of a coastal environment: Flanders Bay, Long Island, New York, *Environ. Sci. Technol.*, *35*, 480–486, 2001.

Moore, W. S., The subterranean estuary: A reaction zone of ground water and sea water, *Mar. Chem.*, *65*, 111–125, 1999.

Officer, C. B., Discussion of the behaviour of nonconservative dissolved constituents in estuaries, *Estuarine Coastal Mar. Sci.*, *9*, 91–94, 1979.

Olsen, H. W., R. W. Nichols, and T. L. Rice, Low gradient permeability measurements in a triaxial system, *Geotechnique*, *35*(2), 145–157, 1985.

Peterson, D. H., R. E. Smith, S. W. Hager, D. D. Harmon, R. E. Herndon, and L. E. Schemel, Interannual variability in dissolved inorganic nutrients in northern San Francisco Bay estuary, *Hydrobiologia*, *129*, 37–58, 1985.

Rivera-Duarte, I., and A. R. Flegal, Pore-water silver concentration gradients and benthic fluxes from contaninated sediments of San Francisco Bay, California, U.S.A., *Mar. Chem.*, *56*, 15–26, 1997a.

Rivera-Duarte, I., and A. R. Flegal, Porewater gradients and diffusive benthic fluxes of Co, Ni, Cu, Zn, and Cd in San Francisco Bay, *Croatica Chem. Acta*, *70*(1), 389–417, 1997b.

Robinson, M., D. Gallagher, and W. Reay, Field observations of tidal and seasonal variations in ground water discharge to tidal estuarine surface water, *Ground Water Monit. Rem.*, *18*(1), 83–92, 1998.

Rowe, P. W., and L. Barden, A new consolidation cell, *Geotechnique*, *16*, 162–170, 1966.

Sañudo-Wilhelmy, S. A., and A. R. Flegal, Trace metal concentrations in the surf zone and in coastal waters off Baja California, Mexico, *Environ. Sci. Technol.*, *30*, 1575–1580, 1996.

Sañudo-Wilhelmy, S. A., K. A. Olsen, J. M. Scelfo, T. D. Foster, and A. R. Flegal, Trace metal distributions off the Antarctic Peninsula in the Weddell Sea, *Mar. Chem.*, *77*(2–3), 157–170, 2002.

Smith, G. J., and A. R. Flegal, Silver in San Francisco Bay estuarine waters, *Estuaries*, *16*(3A), 547–558, 1993.

Sundby, B., L. G. Anderson, P. O. J. Hall, A. Iverfeldt, M. M. Rutgers van der Loeff, and S. F. G. Westerlund, The effect of oxygen on release and uptake of cobalt, manganese, iron, and phosphate at the sediment-water interface, *Geochim. Cosmochim. Acta*, *50*, 1281–1288, 1986.

Treasher, R. C., Geology of the sedimentary deposits in San Francisco Bay, California, *Calif. Div. Mines Geol. Spec. Rep.*, *82*, 11–24, 1963.

Tryon, M., and K. M. Brown, Results from long-term aqueous flux measurements on the Costa Rican convergent margin, *Eos Trans.*, *81*(48), Fall Meet. Suppl., F1161, 2000.

Tryon, M. D., K. M. Brown, M. E. Torres, A. M. Trehu, J. McManus, and R. W. Collier, Measurements of transience and downward fluid flow near episodic methane gas vents, Hydrate Ridge, Cascadia, *Geology*, *27*(12), 1075–1078, 1999.

Tryon, M. D., K. M. Brown, L. Dorman, and A. Sauter, A new benthic aqueous flux meter for very low to moderate discharge rates, *Deep Sea Res., Part I*, *48*(9), 2121–2146, 2001.

Uchiyama, Y. J., K. Nadaoka, P. Rolke, K. Adachi, and H. Yagi, Submarine groundwater discharge into the sea and associated nutrient transport in a sandy beach, *Water Resour. Res.*, *36*(6), 1467–1479, 2000.

Ullman, W. J., and R. C. Aller, Diffusion coefficients in nearshore sediments, *Limnol. Oceanogr.*, *27*(3), 552–556, 1982.

Valiela, I., J. Costa, K. Foreman, J. M. Teal, B. Howes, and D. Aubrey, Transport of groundwater-borne nutrients from watersheds and their effects on coastal waters, *Biogeochemistry*, *10*, 177–197, 1990.

van Geen, A., and S. N. Luoma, A record of estuarine water contamination from the Cd content of foraminiferal tests in San Francisco Bay, California, *Mar. Chem.*, *64*, 57–69, 1999.

Von Herzen, R., and A. E. Maxwell, The measurement of thermal conductivity of deep-sea sediments by a needle-probe method, *J. Geophys. Res.*, *64*(10), 1557–1563, 1959.

Wang, K., and E. E. Davis, Theory for the propagation of tidally induced pore pressure variations in layered subseafloor formations, *J. Geophys. Res.*, *101*(B5), 11,483–11,495, 1996.

Webster, I. T., P. R. Teasdale, and N. J. Grigg, Theoretical and experimental analysis of peeper equilibration dynamics, *Environ. Sci. Technol.*, *32*, 1727–1733, 1998.

Wen, L.-S., P. Santschi, G. Gill, and C. Paternostro, Estuarine trace metal distribution in Galveston Bay: importance of colloidal forms in the speciation of the dissolved phase, *Mar. Chem.*, *63*, 185–212, 1999.

Wheat, C. G., and R. E. McDuff, Mapping the fluid flow of the Mariana Mounds off-axis hydrothermal systems: Pore water chemical tracers, *J. Geophys. Res.*, *100*, 8115–8131, 1995.

Wheat, C. G., and M. J. Mottl, Hydrothermal circulation, Juan de Fuca Ridge eastern flank: Factors controlling basement water composition, *J. Geophys. Res.*, *99*, 3067–3080, 1994.

Wheat, C. G., and M. J. Mottl, Composition of pore and spring waters from Baby Bare: Global implications of geochemical fluxes from a ridge flank hydrothermal system, *Geochim. Cosmochim. Acta*, *64*(4), 629–642, 2000.

Wheat, C. G., J. McManus, J. Dymond, R. Collier, and M. Whiticar, Hydrothermal fluid circulation through the sediment of Crater Lake, Oregon: Pore water and heat flow constraints, *J. Geophys. Res.*, *103*, 9931–9944, 1998.

Wheat, C. G., H. W. Hannasch, J. N. Plant, C. L. Moyer, F. J. Sansone, and G. M. McMurtry, Continuous sampling of hydrothermal fluids from Loihi Seamount after the 1996 event, *J. Geophys. Res.*, *105*, 19,353–19,367, 2000.

Woessner, W. W., and K. E. Sullivan, Results of seepage meter and minipiezometer study, Lake Mead, Nevada, *Ground Water*, *22*(5), 561–568, 1984.

Zago, C., G. Capodaglio, S. Ceradini, G. Ciceri, L. Abelmoschi, F. Soggia, P. Cescon, and G. Scarponi, Benthic fluxes of cadmium, lead, copper, and nitrogen species in the northern Adriatic Sea in front of the River Po outflow, Italy, *Sci. Total Environ.*, *246*, 121–137, 2000.

Zelewski, L. M., D. P. Krabbenhoft, and D. E. Armstrong, Trace metal concentrations in shallow ground water, *Ground Water*, *39*(4), 485–491, 2001.

K. M. Brown and M. D. Tryon, Scripps Institution of Oceanography, University of California, San Diego, La Jolla, CA 92037, USA.

A. T. Fisher and G. A. Spinelli, Earth Sciences Department, University of California, Santa Cruz, CA 95064, USA. (spinelli@es.ucsc.edu)

A. R. Flegal, Environmental Toxicology Department, University of California, Santa Cruz, CA 95064, USA.

C. G. Wheat, Global Undersea Research Unit, University of Alaska Fairbanks, Fairbanks, AK 99701, USA.